Proposed concept

V1

H1 independently broadcasts trajectory and intention to the cloud, which is accessible to V1 and others in real time

H1

Expected outcome

V2

V3

V1

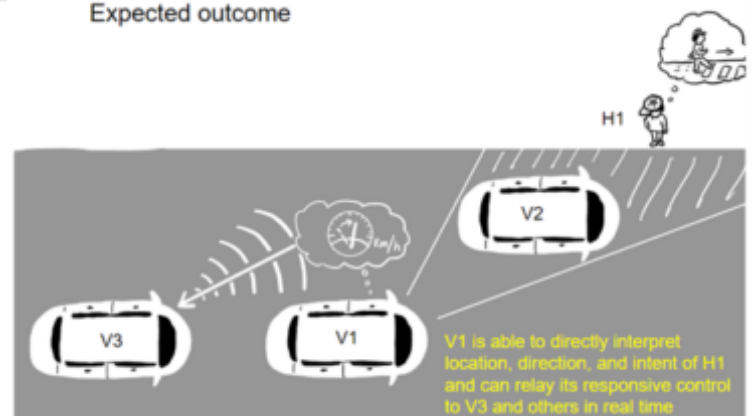V1 is able to directly interpret location, direction, and intent of H1 and can relay its responsive control to V3 and others in real time

H1

COVERT: Cognitive Internet of Vulnerable Road Users in Traffic

Vineet R. Kamat

Carol C. Menassa

Xiaoshan Zhou

COVERT:
Cognitive Internet of Vulnerable Road Users in Traffic

by
Vineet R. Kamat, Professor of Civil and Environmental Engineering
Carol C. Menassa, Professor of Civil and Environmental Engineering
Xiaoshan Zhou, Ph.D. Candidate in Civil Engineering
University of Michigan

DISCLAIMER

Suggested APA Citation: Kamat, V. R., Menassa, C. C., Zhou, X. (2025). COVERT: Cognitive Internet of Vulnerable Road Users in Traffic. Final Report.

DOI: https://doi.org/10.7302/27982

Contacts

For more information:

Vineet R. Kamat
2350 Hayward St.
Ann Arbor, MI 48109
Phone: (734) 764-8495
Email: vkamat@umich.edu

Carol C. Menassa
2350 Hayward St.
Ann Arbor, MI 48109
Phone: (734) 764-8495
Email: menassa@umich.edu

CCAT
University of Michigan Transportation Research Institute
2901 Baxter Road
Ann Arbor, MI 48152
umtri-ccat@umich.edu
(734) 763-2498

Technical Report Documentation Page

1. Report No. Final Report #110	2. Government Accession No.	3. Recipient's Catalog No.
4. Title and Subtitle COVERT: Cognitive Internet of Vulnerable Road Users in Traffic DOI: https://doi.org/10.7302/27982		**5. Report Date** December 18, 2025
		6. Performing Organization Code
7. Author(s) Vineet R. Kamat, Ph.D., https://orcid.org/0000-0003-0788-5588 Carol C. Menassa, Ph.D., https://orcid.org/0000-0002-2453-0386 Xiaoshan Zhou, https://orcid.org/0000-0002-7684-6446		**8. Performing Organization Report No.**
9. Performing Organization Name and Address Center for Connected and Automated Transportation University of Michigan Transportation Research Institute 2901 Baxter Road Ann Arbor, MI 48109 University of Michigan, Department of Civil and Environmental Engineering, 2350 Hayward St., Ann Arbor, MI 48109		**10. Work Unit No.**
		11. Contract or Grant No. Contract No. 69A3551747105
12. Sponsoring Agency Name and Address U.S. Department of Transportation Office of the Assistant Secretary for Research and Technology 1200 New Jersey Avenue, SE Washington, DC 20590		**13. Type of Report and Period Covered**
		14. Sponsoring Agency Code OST-R
15. Supplementary Notes Conducted under the U.S. DOT Office of the Assistant Secretary for Research and Technology's (OST-R) University Transportation Centers (UTC) program.		

16. Abstract

Pedestrians who cross roads, often emerge from occlusion (i.e., obstructed views) or abruptly begin crossing from a standstill, frequently leading to unintended collisions with vehicular traffic that result in accidents and interruptions. Existing studies have predominantly relied on external network sensing and observational data to anticipate pedestrian motion. However, these methods are post hoc (reactive) and insufficient when pedestrians are occluded or stationary, reducing the vehicles' ability to respond in a timely manner. This study addresses these gaps by introducing a novel data stream and analytical framework derived from pedestrians' wearable electroencephalogram (EEG) signals to predict motor planning in road crossings. Experiments were conducted where participants were embodied in a visual avatar as pedestrians and interacted with varying traffic volumes, marked crosswalks, and traffic signals. To understand how human cognitive modules flexibly interplay with hemispheric asymmetries in functional specialization, we analyzed time-frequency representation and functional connectivity using collected EEG signals and constructed a Gaussian Hidden Markov Model to decompose EEG sequences into cognitive microstate transitions based on posterior probabilistic reasoning. Subsequently, datasets were constructed using a sliding window approach, and motor readiness was predicted using the K-nearest Neighbors algorithm combined with Dynamic Time Warping. Results showed that high-beta oscillations in the frontocentral cortex achieved an Area Under the Curve of 0.91 with approximately a 1-second anticipatory lead window before physical road crossing movement occurred. These preliminary results signify a transformative shift towards pedestrians proactively and automatically signaling their motor intentions to autonomous vehicles within intelligent vehicle-to-everything (V2X) systems. The proposed framework is also adaptable to various human-CAV interactions (e.g., bicyclists in traffic), enabling seamless collaboration in dynamic and connected traffic environments.

17. Key Words		18. Distribution Statement		
Motor Readiness; Pedestrian road-crossing; Electroencephalogram (EEG); Hidden Markov Model; Human-Vehicle Interaction; V2X		No restrictions.		
19. Security Classif. (of this report)	**20. Security Classif. (of this page)**		**21. No. of Pages**	**22. Price**
Unclassified	Unclassified		29	Leave blank – not used

Form DOT F 1700.7 (8-72) Reproduction of completed page authorized

Table of Contents

List of Figures

List of Tables

1 Introduction

Pedestrians are among the most vulnerable road users (VRUs) when navigating vehicular traffic, largely due to their increased susceptibility to injury in collisions (Valos & Bennett, 2023). This heightened vulnerability arises from their lower visibility to drivers and the lack of protective structures that could shield them from vehicle impacts. As a result, pedestrians face a significantly higher risk of harm compared to other road users (Anaya et al., 2014). Statistics from the US Governors Highway Safety Association indicate that over 7500 pedestrians were killed in road accidents in 2022, marking the highest number in the past 40 years (Kim, 2023). Similarly, in 2019, 16.1 million road injuries were reported in China, with pedestrian incidents accounting for more than half of the recorded data (Dong et al., 2023). The World Health Organization also reports that more than half of all road traffic deaths involve VRUs, including pedestrians, cyclists and motorcyclists, making pedestrian safety a truly global concern (WHO, 2023).

1.1 Problem Statement and Project Scope

A significant concern regarding pedestrian safety arises when individuals enter the roadway, particularly during the act of crossing. At this point, pedestrians occupy the same space as oncoming traffic (Markkula et al., 2020), thereby increasing the likelihood of path conflicts between pedestrian movements and vehicular flow, which consequently increases the risk of collisions. This safety issue is particularly pronounced in two common situations. The first occurs when pedestrians unexpectedly emerge from drivers' blind spots (Frampton & Millington, 2022; Mole & Wilkie, 2017). Pedestrians may start from locations obscured from a driver's view due to various obstructions, such as emerging from between parked cars, crossing in front of or behind large buses or trucks, being hidden by overgrown trees near intersections or driveways, obscured by street artifacts like large mailboxes or waste receptacles, or hidden behind temporary construction barriers and equipment. These obstructions can prevent pedestrians from being seen by drivers in adjacent lanes. Consequently, when pedestrians suddenly step into the roadway, their unexpected appearance leaves drivers with limited time to perform effective maneuvers or braking to avoid collisions or reduce their impact (Puga et al., 2023).

The second challenging situation is the difficulty in predicting whether and when pedestrians waiting by the roadside will initiate crossing (Rasouli et al., 2018). This uncertainty makes it hard for drivers to respond appropriately, especially on unsignalized roads (those without traffic signals or marked road crossings), where pedestrians may risk jaywalking (Papadimitriou et al., 2016). Pedestrians typically assess traffic volume, speed and the distance to vehicles, then choose a moment they perceive as safe to initiate crossing (Schmidt & Färber, 2009; Sucha et al., 2017). Even at signalized intersections, when the wait time exceeds expectations, pedestrians often cross the road against traffic signals (Kumar & Ghosh, 2022; Lipovac et al., 2013). This behavior is highly unpredictable and abrupt (Ridel et al., 2018). In fact, pedestrians often display impatience and commit traffic violations in their road-crossing behaviors (Ghomi & Hussein, 2022; Kalantarov et al., 2018).

This disregard for traffic rules makes it hard for drivers to interpret the right-of-way and slow down in time to avoid collisions. On the other hand, in those situations where the "yield to pedestrians" rule is not strongly enforced, it is reported that only 34% of drivers yield (Wang et al., 2021). Even at marked crosswalks, 36% of drivers still do not stop and give way to pedestrians (Fu et al., 2018). It is inferred that when it is unclear when pedestrians will start to cross the road, drivers often take risky actions instead of yielding, which greatly increases the chances of accidents occurring.

As autonomous vehicles (AVs) continue to evolve with the vision of enhancing safety and sustainability (Huang et al., 2021), the ability to accurately predict pedestrian movements becomes increasingly critical to ensure that AVs can operate safely and effectively (Almodfer et al., 2015). Unlike human drivers who can often communicate their intentions with pedestrians using eye contact or gestures (Rothenbücher et al., 2016), AVs lack this intuitive form of interaction, making human-vehicle communication significantly more challenging.

Therefore, to avoid collisions and ethical dilemmas in protecting pedestrians, a proactive strategy is to focus on the upstream decision-making points (Kuipers, 2020), which necessitates the forecasting of pedestrians' future motions and trajectory changes (Deshmukh et al., 2023; Goldhammer et al., 2018).

Without accurate prediction of pedestrians' intended movement and considering the additional complexity of pedestrians sometimes being invisible to sensors, the safe operation of AVs and their acceptance by the public become more difficult and raise further concerns (Chavhan et al., 2023; Keller & Gavrila, 2014).

1.2 Limitations of Existing Methods in Pedestrian Trajectory Prediction
1.2.1 Cooperative Sensing Between Vehicular Communication Modes
To overcome the challenge of occlusion (view blocked by objects), current research recommends using cooperative sensing within Vehicle-to-Vehicle and Vehicle-to-Infrastructure frameworks (Malik et al., 2023). In this approach, cameras mounted on other vehicles or traffic infrastructure offer different viewpoints to detect the location and movement of pedestrians (Koda et al., 2020; Tang et al., 2021). This information is then shared with approaching vehicles that cannot see the pedestrians due to blind spots (Wang et al., 2020), allowing them to coordinate actions to keep a safe distance (Flores et al., 2019; Koopmann et al., 2020).

This approach relies on communication between connected agents within the intelligent transportation system, offering a viable solution for smart intersections and dense urban areas (Moradi-Pari et al., 2022). However, in suburban areas where there are fewer vehicles to provide alternative viewpoints or where there are unsignalized crosswalks without street cameras, this occlusion problem cannot be fully resolved. In addition, even when pedestrians are visible, the dependence on vision-based methods for sensing has certain limitations, which are discussed in detail below.

1.2.2 Vision-based Methods for Predicting Pedestrians' Future Movements
In vision-based methods where road security cameras (Noh et al., 2021) or stereo-based cameras installed in passenger vehicles (Keller & Gavrila, 2014) are leveraged to detect pedestrians (Gandhi & Trivedi, 2007), extract their behavioral features from video footage (Noh et al., 2022), and analyze collision risks between pedestrians and vehicles (Matsui et al., 2013), there are typically three primary analytical approaches:

1) Dynamic Motion Modelling: One research stream treats the prediction for VRU intentions as a dynamical motion modeling problem, often addressed using Bayesian filters (Pool et al., 2017; Schneider & Gavrila, 2013). These approaches require explicit modeling of agents, and while effective in specific traffic scenarios (Song et al., 2020), they struggle with non-linear motion trajectories and the tracking dynamics over longer periods where increased uncertainty arises in path changes due to complex interactions inherent in real-word traffic.

2) Planning-based Models: Another research direction explores planning-based models for forecasting pedestrians' trajectories. These models use end goals and occupancy grid maps of the environment to generate a probability distribution over possible trajectories (Bandyopadhyay et al., 2013; Rehder & Kloeden, 2015). Although planning-based approaches do not require explicit modeling of motion dynamics, their effectiveness is constrained by their dependence on a prior knowledge of the pedestrians' end goals.

3) Deep learning methods: The third stream of studies incorporates deep learning techniques, such as three-dimensional pose estimation of pedestrians (Kim et al., 2020) (including head movement (Lyu et al., 2024) and body skeleton (Jiang et al., 2022)) and recurrent neural network-based methods that use past positions to predict future motion trajectories (Alahi et al., 2016; Saleh et al., 2017; Saleh et al., 2018). Additionally, some models integrate contextual environmental information, such as the pedestrian's distance to the curb and the relative locations of nearby approaching vehicles, to enhance the prediction of road-crossing intentions (Neogi et al., 2020; Saleh et al., 2019).

These deep learning methods can achieve favorable results under clear visibility, good weather, and adequate lighting conditions. However, their reliance on sensors such as cameras, LiDAR, and radar introduces several limitations. These sensors are subject to constraints in range, resolution, and accuracy (Yeong et al., 2021), and they are particularly susceptible to noise and measurement errors under adverse lighting (e.g., low light or direct sunlight) and weather conditions (e.g., fog, heavy rain, or snow) (Pang et

al., 2021; Swargiary & Kadali, 2023). Although advanced sensor fusion techniques can enhance sensor measurements (Volz et al., 2016), they are often cost-prohibitive and computationally intensive, with data processing requirements reaching up to 5TB per hour (Rich, 2020).

Another significant limitation is that although explicit representations of pedestrian behaviors (such as past positions and skeletal poses) can effectively predict future trajectories and road crossing intentions when pedestrians are in motion, it becomes challenging to accurately predict the exact moment pedestrians will initiate road crossing once they are standing at the curb without a clear intention to cross (Rasouli et al., 2018).

1.2.3 Pedestrians as Data Source

A cooperative approach has been proposed wherein pedestrians themselves can exchange information with vehicles, augmenting the vehicle's sensor capabilities. Smartphone and wearable sensors on pedestrians are typically leveraged to enhance pedestrian localization and movement prediction. For instance, one study employed GPS in smartphones to provide precise pedestrian location information, thereby reducing reliance on external cameras for position estimation (Liebner et al., 2013). Another study incorporated accelerometers in mobile phones to detect changes in pedestrian movements, enhancing tracking accuracy (Flach et al., 2011). Similarly, inertial smartphone sensors have been used to detect pedestrian turning or crossing an intersection (Datta et al., 2014).

Moreover, wearable inertial measurement units mounted on the human body facilitate accurate pedestrian localization (Harle, 2013). Pressure-sensitive mats or insoles placed on the feet gather data on gait characteristics, such as stride length (Gao et al., 2016). The motion of body segments and joints is analyzed to understand the mechanics of walking, with kinematic models simulating human gait and predicting future movements. Additionally, radio signal propagation methods have been used to calculate the precise distance between vehicles and pedestrians (Andreone et al., 2006). Despite the increased positional accuracy provided by these approaches, they are largely reactive rather than proactive, i.e., they detect post-hoc behavioral patterns that have already occurred. For predicting the initiation of road-crossing by pedestrians, these methods fail to provide connected vehicles sufficient advance notice to respond in time.

Some other researchers have explored empowering pedestrians to act as active beacons for their planned road crossing. One particular study investigated using smartphones to notify nearby AVs about pedestrian positions, proposing a system architecture for pedestrian-to-vehicle communication (Arena et al., 2019). This system further calculates collision risk and triggers alarms if necessary (Sugimoto et al., 2008). However, this notification process is not automatic, requiring pedestrians to actively engage with these third-party applications, which significantly limits its real-world adoption. This additional effort reduces the practicality of such systems and poses barriers to accessibility, particularly for vulnerable populations, such as older adults and persons with disabilities.

1.4 Project Objective

This project aims to explore the feasibility of an automatic prediction approach for pedestrian road-crossing initiation based on continuously monitored brain activities captured by a wearable, non-invasive EEG device. Given the complex spectral-spatial-temporal characteristics of EEG signals and the ever-increasing compactness and wearability of EEG devices (Sharma et al., 2022), the novelty and points of departure of this study are as follows:

1) This is the first study in our domain to use scalp EEG recording alongside source localization and brain connectivity analysis to investigate neural activation in deeper brain structures and functional coordination between different brain regions, providing new insights into cognitive processes.

2) To the best of our knowledge, this is the first study to investigate motor planning while developing a computational approach—combining statistical dependency analysis and machine learning—to model the temporal evolution of underlying neural modulation for predicting motor readiness. The ability to capture temporal dependencies in fast-evolving EEG patterns is critical and adaptable to many real-time and high-level decision-making tasks in human-robot interactive systems, moving beyond traditional EEG

studies focused on emotional and stress states that change slowly over seconds or minutes.

3) This is the first study that examines motor readiness in a real-life decision-making context within a perception-action loop, where movement decisions are made dynamically based on perceptions of environmental cues and interactions with other entities. This study moves beyond reactive sensing to predictive (embodied perception) modeling and optimizes sliding window length and stride to provide critical lookahead time. These findings can be applied to connected vehicles and adapted for assistive and industrial robots, enabling them to understand human motion intentions and make intelligent decisions about path coordination and handovers in both non-interaction and seamless collaborative settings.

2 Technical Approach
2.1 EEG Applications and Technical Gaps

Electroencephalography (EEG) measures brain electrical activity resulting from the flow of electric currents during synaptic excitations of neuronal dendrites via electrodes placed on the scalp (Abiri et al., 2019; Anwar et al., 2017). EEG was originally used as a neuroimaging tool and for monitoring subject's mental states, such as emotions in interpersonal interactions (Gannouni et al., 2021), mental workload in employees (Chen et al., 2016; Eoh et al., 2005). EEG has also been used in brain-computer interface (BCI) systems to provide a direct communication pathway from the human brain to manipulate external devices, such as neuroprosthetic and neurorehabilitation tools (e.g. wheelchair, robotic arms). These applications are particularly beneficial for physically disabled individuals, including paralyzed patients, amputees, and individuals recovering from brain injuries (e.g. stroke patients) (Abiri et al., 2019). In recent years, EEG applications have gained increasing significance beyond the medical domain (see (Värbu et al., 2022) for an overview). Emerging applications include controlling smart home devices (Gao et al., 2018), thought-controlled vehicle (Lu & Bi, 2019), game control for entertainment (Liao et al., 2012), enhancing creativity in education (Yin et al., 2024), identity authentication (Bidgoly et al., 2022), music recommendation systems (Cui et al., 2022).

Previous EEG studies in the civil infrastructure community have primarily focused on assessing cognitive state as physiological measures, typically inducing specific mental states in controlled experimental settings, linking them to the tasks being performing (Chauhan et al., 2024) or the contexts being experienced (Ergan et al., 2019; Zou et al., 2021), and using supervised learning models to classify different states or exogenous tasks (Jiang et al., 2024). Although these approaches provide insights into static cognitive states, they fail to capture the temporal evolution of cognitive processes. For higher-level cognitive tasks, particularly those involving complex perceptual decision-making, cognitive processing is dynamic and continuously evolving. Although a few studies suggest that the brain actively reconfigures neural resources across different time scales and modulates ocular activities for scanning and information-seeking behavior (Liao et al., 2022; Zhang et al., 2023), there is no established method to track these dynamics over time.

On the other hand, motor preparedness (or readiness) has been extensively studied in the psychology and neuroscience communities (Parés-Pujolràs et al., 2023). Research has found neural correlates of decision-making in the Frontal Eye Field of mammal animals, both before, during, and after decision commitment. These findings are consistent with the temporal accumulation of sensory evidence, where neural activities modulates till convergence to a threshold before triggering a behavioral response (Ding & Gold, 2011). Studies have also identified the readiness potential as an event-related potential (ERP) that signals an upcoming action. This potential precedes subjects' reports of their decision to move, but crucially, it is more prominent in unconscious or spontaneous actions. In other words, it does not exhibit strong modulations in deliberate, reasoning-based decisions (Maoz et al., 2019). This limitation suggests that the readiness potential cannot serve as a direct neural proxy for predicting upcoming road-crossing actions, unlike more well-established ERPs such as P300 or error-related potential, which have been widely used in BCI applications (Salazar-Gomez et al., 2017; Yu et al., 2017). Instead, alternative neural markers in the frequency domain may provide stronger predictive value. For instance, research has shown that beta-band event-related desynchronization (ERD) is closely linked to prospective conscious access to motor preparation (Parés-Pujolràs et al., 2023). Donner et al. (2009) found that beta-frequency range (12–30 Hz)

in the motor cortex can predict participants' perceptual choices in a yes-or-no visual detection task, before their overt manual responses (Donner et al., 2009). These neurophysiological findings provide insights into potential neural signatures of movement-related decision-making. However, substantial empirical evidence is needed to validate these findings in more complex perceptual decision-making and assess their computational feasibility for motor preparedness prediction.

2.2 Overview of the Developed Computing Framework

An overview of the computational framework proposed in this study is shown in Figure 1. The details are provided in the following subsections.
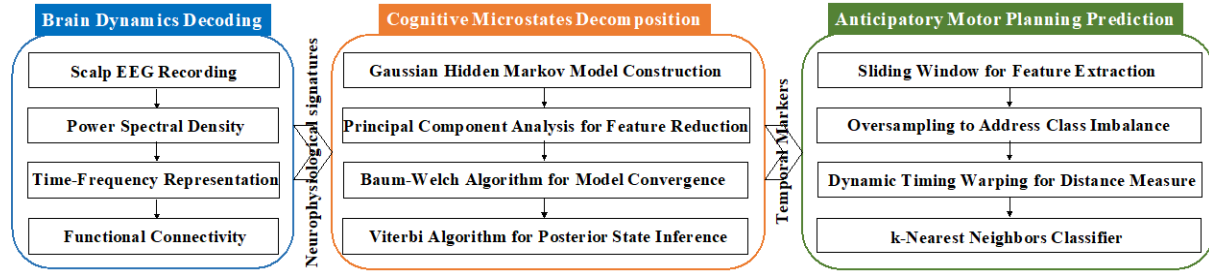

Figure 1. Overview of the computing framework.

2.3 Power Spectral Density

EEG data were recorded as voltage fluctuations over time (time domain). Fast Fourier Transform (FFT) (Cochran et al., 1967) was performed to transform the signal into frequency domain that decomposed the EEG signals into five frequency components: theta (4–8 Hz), alpha (8–12 Hz), low beta (12–16 Hz), high beta (16-25Hz) and gamma (25–45 Hz). A Hanning tapered window was used to prevent wrapping artefacts, which occur when the FFT treats the data as an infinite repeating sequence. Without tapering, any mismatch between the first and last samples would be interpreted as a sudden jump, introducing spectral leakage—artificial noise broadcast across the frequency spectrum. This analysis was conducted by the EmotivPRO software (v3.0) (EMOTIV, 2023). The FFT outputs ($X(f)$) contains both magnitude and phase information about different frequency components of the signals. Later, the squared magnitude of $X(f)$ was computed as power spectrum and normalized by the frequency resolution (Δf) to obtain Power Spectral Density (PSD). Given the 5 frequency bands and 14 electrodes embedded in our scalp recording headset, the PSD data structure had 70 dimensions on a continuous time scale at a sampling rate of 8Hz.

2.4 Epoch Segmentation

Epoch segmentation was performed using event markers corresponding to stimuli onset and participant responses to extract stimulus-response period-of-interest. Epochs were segmented on a trial-by-trial basis and labeled according to the experimental scenario. Both EmotivPro (for EEG data) and PsychoPy (for experimental stimuli) generated marker/event files (.csv) that contains timestamp information. However, these timestamps were recorded in different local time scales, making direct alignment challenging. To synchronize, Psychopy was programmed to send event triggers directly to the Emotiv EEG recording system, ensuing that both datasets contained a shared reference timestamp for stimulus onset. This shared timestamp was then used as an index reset point.

2.5 Time-Frequency Analyses

PSD provides an average power distribution across different frequency over the entire epoch segment, but it does not retain temporal information. To get a dynamic view of power fluctuations at different frequencies over time, time-frequency analysis was performed. Given the inherent time-frequency trade-off—where longer temporal windows improve frequency resolution but reduce temporal precision, while shorter windows enhance time resolution but cause frequency smearing (MNE-Python)—two methods were

applied: Morlet wavelet transform that uses sinusoidal waves multiplied by a Gaussian envelope to convolve the signal and localize in time, which provides good time resolution but lower frequency resolution, and a multitaper method that uses multiple orthogonal tapering windows to compute independent spectral estimates and average them, which reduces variance and provides high frequency resolution but is limited in temporal precision (Slepian, 1978).

The reason to perform time-frequency analysis and the differences between ERP and ERD or event-related synchronization (ERS) can be found in (Pfurtscheller & Lopes da Silva, 1999). Traditional ERP analysis relies on trial averaging, which enhances phase-locked signals but filters out non-phase-locked activity. However, event-related oscillations—frequency-specific changes in ongoing EEG activity triggered by an event—may not be phase-locked, meaning they could be lost in ERP averaging but remain detectable using time-frequency analysis. In time-frequency analysis, the power dynamics of frequency-specific oscillations are quantified over time, enabling the examination of how spatiotemporal changes in EEG activity relate to task-specific sensory, motor, and/or cognitive processes. A decrease in power within a specific frequency band indicates ERD (Pfurtscheller, 1977), reflecting a reduction in neuronal synchrony, often associated with increased cortical activation or engagement. Conversely, an increase in power is referred to as ERS (Pfurtscheller, 1992), indicating greater neuronal synchrony, often linked to functional inhibition or memory processes.

The EEG data were exported from EmotivPro in European Data Format (.edf) and processed using MNE-Python (Gramfort et al., 2013) for time-frequency analysis. To visualize event-related power changes, the EEG data was normalized using a 200-millisecond pre-stimulus baseline interval. Two normalization methods were applied: (1) arithmetic mean correction, which corrects bias by subtracting the average power across segments, and (2) log-ratio transformation, which computes the logarithmic ratio of power relative to the baseline mean, providing a scale-invariant measure of power fluctuations.

2.6 Functional Connectivity

Activation-based analysis can identity strong localized activity in specific brain regions; however, the brain operates as a network, where inter-regional coordination plays a crucial role in distributed cognitive processes and synchronized neural dynamics—especially for high-level cognitive functions. Isolated activation patterns alone may not fully capture these interactions (Liao et al., 2022). Therefore, this study also examines functional connectivity to understand how different brain regions interact over time.

The Weighted Phase Lag Index (wPLI) was computed to estimate the synchronization between two brain regions based on phase difference in their oscillatory activity. Suppose S_{ij} is the cross-spectrum (multiplication of one signal's Fourier transform with the complex conjugate of the other) between two signals i, j. wPLI measures the consistency of the imaginary component of the phase difference between these two signals:

$$wPLI = \frac{\left| E\left\{ \text{Imag}\left(S_{ij} \right) \right\} \right|}{E\left\{ \text{Imag}\left(\left| S_{ij} \right| \right) \right\}}$$

where $E\{*\}$ denotes the expectation across time/frequency epochs.

When neurons generate electrical activity, the signals propagate through brain tissue, cerebrospinal fluid, the skull, and the scalp before being captured by EEG electrodes. Because the brain's electrical activity spreads through these conductive media, two electrodes may pick up the same signal from a common source, creating the false appearance of connectivity—a phenomenon known as volume conduction. wPLI helps mitigate volume conduction, compare to traditional connectivity measures such as coherence and Phase-Locking Value (PLV). wPLI focuses only on non-zero phase lags: the imaginary component of the cross-spectrum is maximal when signals have a phase difference of $k\pi + \frac{\pi}{2}$ and zero

when the phase difference is $k\pi$ (where $k \in \mathbb{Z}$) (Vinck et al., 2011). wPLI is bounded in the range of $[0, 1]$, where higher values indicate stronger phase synchronization with a consistent lag.

2.7 Hidden Markov Models for Decomposing Microstates

Based on the Perception-Action model (Kowalski-Trakofler & Barrett, 2003; Windridge et al., 2013), we hypothesized that there are four key cognitive microstates underlying the road-crossing decision (Tian et al., 2022): perceiving the environment (selectively attending to critical sensory information, such as oncoming traffic), assessing risk based on vehicle speed and distance, determining the available time to cross, and initiating movement onto the road. These processes are complex and engage multiple high-level functions, such as selective attention, which orients focus on highly relevant environmental cues (Ptak, 2012), and working memory that manipulates information for memory retrieval and rule-based response selection (Bunge, 2005).

To identify temporal markers that distinguish these hypothesized latent cognitive states and their transitions, we constructed a Hidden Markov Model (HMM) to infer these states using probabilistic inference (Rabiner, 1989). In this framework, road-crossing decision-making was modeled as a Markov process with hidden states, which were inferred from multivariate EEG power time series data, leveraging the probabilistic dependence (transition probabilities) of successive hidden states.

To explain the statistical inference process in more details, let $S = \{S_1, S_2, S_3, S_4\}$ be the set of four latent states. The initial state distribution π represents the probability of starting in each state: $\pi = \{\pi_1, \pi_2, \pi_3, \pi_4\}$, where $\pi_i = P(S_1 = S_i)$, for $i \in \{1,2,3,4\}$.

The state transition matrix A represents the probabilities of transitioning from one state to another:

$$A = \begin{bmatrix} a_{11} & a_{12} & a_{13} & a_{14} \\ a_{21} & a_{22} & a_{23} & a_{24} \\ a_{31} & a_{32} & a_{33} & a_{34} \\ a_{41} & a_{42} & a_{43} & a_{44} \end{bmatrix}$$

Equation 2

where $a = P(S_{t+1} = {}_i | S_t = {}_i)$ for $i, j \in \{1,2,3,4\}$.

The emissions from each state are modeled by Gaussian distributions. Each state S_i is associated with a Gaussian distribution characterized by a mean μ_i and a covariance matrix U_i. The estimation probabilities are modelled by

$$B_i = N(\mu_i, U_i)$$

Equation 3

where $N(\mu_i, U_i)$ represents the multivariate Gaussian distribution with mean vector μ_i and covariance matrix U_i.

$$P(O_t | S_t = S_i) = N(O_t | \mu_t = U_i), i \in \{1, 2, 3, 4\}$$

Equation 4

where O_t is the observed data at time t.

The process of estimating these model parameters was performed through a fitting procedure, wherein the model iteratively adjusted the parameters to maximize the likelihood of the observed data given the model structure. The Expectation-Maximization (EM) algorithm, specifically the Baum-Welch algorithm (Fine et al., 1998), is used to train the HMM. After firstly initializing the model parameters π, A, and B, the forward and backward probabilities using the current parameters were calculated:

Forward Probabilities (α):

$$\alpha_t(i) = P(O_1, O_2, ..., O_t, S_t = S_i | \lambda)$$

Equation 5

7

$$\alpha_1(i) = \pi_i b_i(O_1)$$

Equation 6

$$\alpha_{t+1}(j) = \left(\sum_{i=1}^{N} \alpha_t(i) a_{ij} \right) b_j(O_{t+1})$$

Equation 7

Backward Probabilities (β):

$$\beta_t(i) = P(O_{t+1}, O_{t+2}, ..., O_T, S_t = S_i \mid \lambda)$$

Equation 8

$$\beta_T(i) = 1$$

Equation 9

$$\beta_t(i) = \left(\sum_{j=1}^{N} a_{ij} b_j(O_{t+1}) \right) \beta_{t+1}(j)$$

Equation 10

Then the model parameters were updated to maximize the expected likelihood. The initial state distributions were re-estimated:

$$\pi_i = \gamma_1(i)$$

Equation 11

where $\Upsilon_t(i) = P(S_t = S_i | O, \lambda)$ and can be computed as:

$$\gamma_t(i) = \frac{\alpha_t(i)\beta_t(i)}{\sum_{j=1}^{N} \alpha_t(j)\beta_t(j)}$$

Equation 12

The state transition probabilities were re-estimated:

$$a_{ij} = \frac{\sum_{t=1}^{T-1} \xi_t(i,j)}{\sum_{t=1}^{T-1} \gamma_t(i)}$$

Equation 13

where $\xi(i,j) = P(S_t = S_i, S_{t+1} = {}_i | O, \lambda)$. The emission probabilities were re-estimated:

$$\xi_t(i,j) = \frac{\alpha_t(i) a_{ij} b_j(O_{t+1}) \beta_{t+1}(j)}{\sum_{i=1}^{N} \sum_{j=1}^{N} \alpha_t(i) a_{ij} b_j(O_{t+1}) \beta_{t+1}(j)}$$

Equation 14

For the Gaussian distribution associated with each state S_i:

$$\mu_i = \frac{\sum_{t=1}^{T} \gamma_t(i) O_t}{\sum_{t=1}^{T} \gamma_t(i)}$$

Equation 15

$$U_i = \frac{\sum_{t=1}^{T} \gamma_t(i)(O_t - \mu_t)(O_t - \mu_t)^T}{\sum_{t=1}^{T} \gamma_t(i)}$$

<div align="right">*Equation 16*</div>

This iterative process continued until convergence (i.e., the change in likelihood between iterations is below a certain threshold), ensuring that the model parameters were optimized to best represent the underlying structure of the EEG data.

Following the optimization of the model parameters, the most probable sequence of hidden states were inferred from the time series of observed data using the Viterbi algorithm. First, the variables for the most probable path up to time t ending in state S_i, denoted as $\delta_t(i)$, and the backpointer $\psi_t(i)$ to keep track of the states were initialized:

$$\delta_1(i) = \pi_i b_i(O_1), \psi_1(i) = 0, i \in \{1,2,3,4\}$$

<div align="right">*Equation 17*</div>

For each time step $t = 2, \ldots, T$ and each state S_j:

$$\delta_t(j) = \max_{i \in \{1,2,3,4\}} \left[\delta_{t-1}(i) a_{ij} \right] b_j(O_t)$$

<div align="right">*Equation 18*</div>

$$\psi_t(j) = \arg \max_{i \in \{1,2,3,4\}} \left[\delta_{t-1}(i) a_{ij} \right]$$

<div align="right">*Equation 19*</div>

The most probable final state and the corresponding probability was identified by:

$$P^* = \max_{i \in \{1,2,3,4\}} \delta_t(i)$$

<div align="right">*Equation 20*</div>

$$S_T^* = \arg \max_{i \in \{1,2,3,4\}} \delta_t(i)$$

<div align="right">*Equation 21*</div>

Then the most probable sequence of states was retrieved by backtracking through the backpointer array $\psi_t(i)$:

$$S_t^* = \psi_{t+1}(S_{t+1}^*), t = T-1, T-2, \ldots, 1$$

<div align="right">*Equation 22*</div>

This sequence, $\{S_1^*, S_2^*, S_3^*, S_4^*\}$ resulted in a temporal map of the latent cognitive microstates experienced by participants during the road-crossing decision-making process.

2.8 Motor Readiness Prediction

To create the dataset for training the machine learning classifier, a sliding window approach was adopted, where a fixed-length window moves over the EEG power data with a specific stride to extract segments from the time series. Depending on the length and stride, the segments could be overlapping or non-overlapping. In this study, an exhaustive search method was used to find the optimal window configuration that results in the best signal classification performance. The length and stride of each window started at 0.25 seconds (s) and incrementally increased by 0.125s at each stop until a maximum of 2s. As a result, the total of windows W extracted from the time series is given by

$$W = \left\lfloor \frac{N-L}{S} \right\rfloor + 1$$

<div align="right">*Equation 23*</div>

where N is the total number of data points, L is the window length, S is the stride. $\lfloor * \rfloor$ denotes the floor function that returns the greatest integer less than or equal to the given value.

The last (W-th) window, ω_W, can be described as:

$$\omega_W = \left\{ x_{t_w}, x_{t_{w+1}}, x_{t_{w+2}}, ..., x_{t_{w+L-1}} \right\}$$

<div align="right">*Equation 24*</div>

This last segment, which reaches the end of the sequence, was assigned a label of "1", signifying the final initiation of road-crossing. The earlier segments were all assigned a label of "0". Given the pronounced class imbalance within the dataset, Adaptive Synthetic Sampling Approach (ADASYN), which was commonly used for oversampling (He et al., 2008), was used to adaptively generate synthetic samples for the minority class.

Based on the segmented dataset, a K-Nearest Neighbors (KNN) classifier was used to predict the precise moments when participants decide to initiate road crossing. Dynamic time warping (DTW) distance between two time series was used as the distance measure. Originally proposed in (Sakoe & Chiba, 1978), DTW is an elastic distance measure, i.e., it is a distance computed after realigning (warping) two time series to best match each other via time axis distortions (Ratanamahatana & Keogh).
This is critical for considering the non-fixed response time across trials, where similar cognitive processes may unfold at different rates. The underlying principal is that DTW compares two time series by optimally aligning their points to minimize the distance between them, thus taking into account the temporal differences in speed or duration between the series.

To be more specific, two sequences that we want to compare are defined below:
- $X = [x_1, x_2, ..., x_n]$ with length n
- $Y = [y_1, y_2, ..., y_m]$ with length m

The goal of DTW is to find a path through the grid that defines the mapping between X and Y that minimizes the total distance between the aligned elements of the sequences. This path is known as the "warping path". First, the distance matrix D was computed, where each element $D(i,j)$ represents the Euclidean distance between x_i and y_j:

$$D(i,j) = \left(x_i - y_j \right)^2$$

<div align="right">*Equation 25*</div>

Next, the accumulated cost matrix C was calculated using dynamic programming. Each element $C(i,j)$ represents the minimum cumulative distance to align the first i elements of X and the first j elements of Y. The accumulated cost matrix is defined as:

$$C(i,j) = D(i,j) + \min\left\{ C(i-1,j-1), C(i-1,j), C(i,j-1) \right\}$$

<div align="right">*Equation 26*</div>

The boundary conditions are:

$$C(0,0) = D(0,0)$$

<div align="right">*Equation 27*</div>

$$C(i,0) = D(i,0) + C(i-1,0), i-1,2,...,n$$

<div align="right">*Equation 28*</div>

$$C(0,j) = D(0,j) + C(0,j-1), j = 1,2,...,m$$

Equation 29

The optimal warping path P is the path from $C(n,m)$ to $C(0,0)$ that minimizes the total cumulative distance. This path is found by starting at $C(n,m)$ and tracing back to $C(0,0)$ by moving through the indices that provide the minimum accumulated cost as defined above. Finally, the total cost of the optimal warping path, which is the measure of similarity between X and Y, is given by the value of $C(n,m)$.

By integrating DTW as the distance metric, our KNN classifier gains the flexibility to accurately measure the similarity between EEG sequences with temporally varying patterns. The KNN algorithm determines the classification of a sample by identifying the majority class among its k closest neighbors. Through tuning, $k = 5$ was chosen. The tslean toolkit that specializes in machine learning for time series analysis in Python was used for this analysis (Tavenard et al., 2020).

The performance of the classifier was assessed based on five-fold cross validation. The dataset was divided into five subsets. In each validation cycle, four subsets underwent ADASYN oversampling to address class imbalance before being used for training, while the fifth subset was used for testing. Each subset of data was used for testing exactly once, and the average of the evaluation metrics across all subsets was calculated and reported. Finally, A permutation test was implemented to evaluate how well the classifier performed by comparing with the observed accuracy obtained by chance (from the datasets where the class labels were randomly shuffled) (Ojala & Garriga, 2009).

3 Experiments
3.1 Participants
Twelve participants were recruited for the experiment (six males and six females; mean age = 24.92 years). This sample size was determined based on the latest biometric review, which reports that prior EEG studies in the civil engineering domain typically recruit an average of 12 participants (Cheng et al., 2022). In addition, the sufficiency of the dataset for the primary modelling approach used in this study–the HMM— was validated by the convergence of model fitting. For statistical analysis, normality assumptions were first tested, followed by effect size reporting, with an effect size of d=0.4 as a reference of minimal acceptable threshold for supporting reliable results in psychological experiments (Brysbaert, 2019). All participants had normal or corrected-to-normal vision and reported no history of neurological health issues, such as epilepsy or brain cancer. They all provided verbal informed consent prior to participation. This study was approved by the University of Michigan Institutional Review Board (Reference ID HUM00249262).

3.2 Stimuli
The stimuli used in the experiment were designed to simulate a variety of real-world traffic conditions and scenarios. As detailed in Table 1, five scenarios were developed with variations in intersection settings and traffic volumes. These scenarios were informed by prior research on pedestrian safety and road-crossing behaviors. Studies highlight that 30% of pedestrian accidents occur at non-signalized crosswalks (Fu et al., 2019; Gerogiannis & Bode, 2024; Haleem et al., 2015; Noh et al., 2020; Olszewski et al., 2015), coupled with different traffic volumes (Alver & Katanalp, 2022). The classification of traffic volumes in our scenarios was guided by three established definitions of roadway density conditions (Homburger et al., 1982). In addition, pedestrian road-crossing intentions have been examined in various intersection contexts (Kim et al., 2020; Koehler et al., 2013; Volz et al., 2016) and in the presence of right-turning vehicles (Kumar et al., 2019). The stimuli, illustrated in Figure 2 (as static images), were crafted using Adobe Animate. The GIF versions of these are available in the supplementary materials. The vehicular flow animations were generated using Motion Tween (Adobe, 2023). The traffic speeds were configured by adjusting the playhead frame on the tween span at a 24 frames per second (FPS) rate. The right-turn flickering signal was created using multiple keyframes with alternative light source invisibility and an overlay layer with reduced opacity to simulate ambient dim lighting. A blur effect with glow was created for the red traffic light to enhance its luminance and visibility.
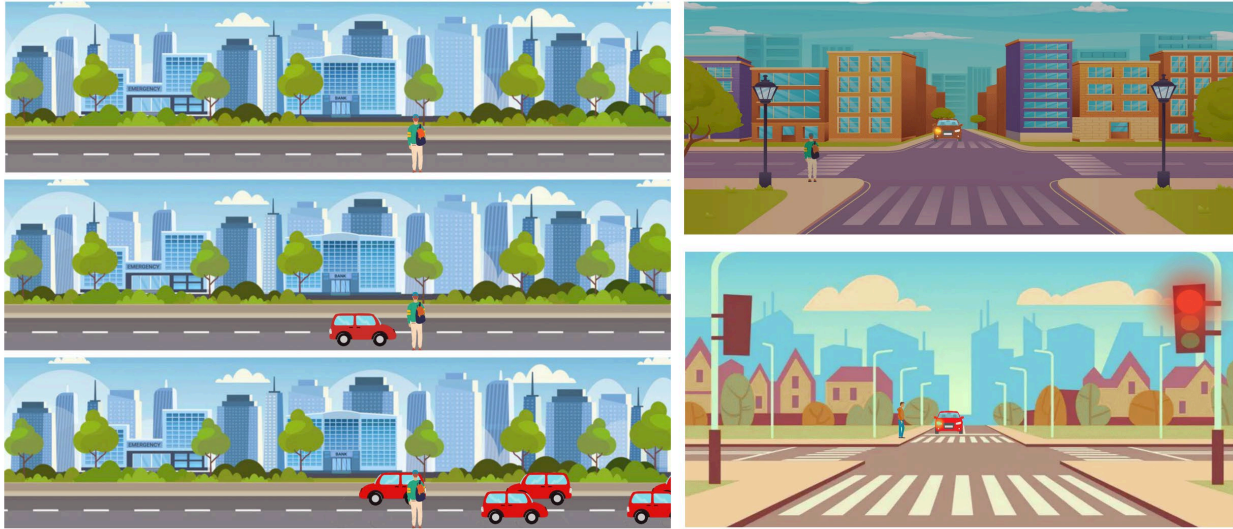
Figure 2. Experimental Stimuli (presented as animations to participants).

Table 1 Descriptions of the simulated experimental scenarios

Traffic Scenarios	Description
Minimal Traffic Volume	A two-lane road without signalized crosswalks, with no cars approaching within sight.
Low Traffic Volume	A two-lane road without signalized crosswalks, with two cars approaching at a slow speed within sight.
High Traffic Volume	A two-lane road without signalized crosswalks, with two cars approaching in the adjacent lane and three vehicles approaching in the opposite lane at a moderate speed within sight.
Surface-marked Intersection	A four-way intersection with surface-marked crosswalks but without traffic lights. One car is waiting behind the sidewalk on the side opposite to the pedestrian's intended movement, with its right-turn signal flashing and visible within sight.
Signalized Intersection	A four-way intersection with surface-marked crosswalks and a traffic light (green/red). One car is waiting behind the sidewalk in the vertical orthogonal direction relative to the pedestrian's intended movement with its right-turn signal flashing. A red traffic light, perpendicular to the pedestrian's movement, is visible at the intersection.

3.3 Experimental Procedure

One day before the experiment, participants received a reminder email detailing the appointment and preparatory requirements, including ensuring a good night's sleep, abstaining from caffeinated beverages, and showering with a mild shampoo before the experiment. The experiment was conducted in a dimly lit and sound-attenuated room. First, participants completed a self-report questionnaire to collect basic demographic information, such as age, gender, and education level. Subsequently, the experimenter helped the participants wear the EEG headset. Saline-soaked felt pads were used for electrode contact. After fitting the headset, the experimenter carefully separated hair from each electrode to ensure adequate scalp contact and rehydrated the sensor felts as necessary. The contact quality (impedance) of each electrode was continuously monitored via the EmotivPro software (EMOTIV, 2023). Recording of EEG signals started only after confirming that all electrodes maintained good contact quality.

The procedure for each trial was described as follows: Each trial began with a 500-millisecond fixation cross (+) to calibrate participants' attention to the center of the screen. Subsequently, a video clip simulating a road-crossing scenario was played. Participants were asked to envision themselves as the pedestrian standing beside the road curb. Their task was to perceive the traffic flow and determine the safest moment to cross the road. When they decided it was the right moment to cross, they pressed the "up" key on the keyboard. Participants were self-paced with no time pressure to make a decision. Each animation continued looping until the participant responded. The program then automatically proceeded to the next scenario.

After completing all of five scenarios participants were asked to provide retrospective "thinking aloud" to reflect on their perceptions and decision-making process in each of the five scenarios. These verbal statements were recorded.

3.4 EEG Signals and Event Markers Recording

EEG signals were recorded using a 14-electrode headset (EPOC X, Emotiv), which was placed according to the international 10-20 system (Klem et al., 1999) at a sampling rate of 128Hz. During the recording, a 0.16Hz first order high-pass filter was used to remove the DC offset. The 14 electrodes and their corresponding cortical regions are: the frontal region (AF3, F7, F3, F4, F8, AF4), responsible for executive functions including decision-making, problem-solving, and planning (Chayer & Freedman, 2001; Frith &

Dolan, 1996); the central region (FC5, FC6), implicated in integrating sensory and motor information (Liao et al., 2022); the parietal region (P7, P8), key to spatial awareness and processing of visual and somatosensory data (Bressler et al., 2008); the temporal region (T7, T8), essential for semantic processing and memory functions (Schrouff et al., 2020); and the occipital region (O1, O2), dedicated to visual processing (Shokri-Kojori et al., 2012). A picture of participants wearing the EEG headset is shown in Figure 3.

Figure 3. Participants wearing the EEG headset in the experiment.

The stimuli were presented to participants using PsychoPy (v2022.2.5) (Peirce et al., 2019). The program automated the experiment and ensured that each participant experienced the same sequence of stimuli, timing and conditions. Furthermore, Psychopy includes built-in plugins for synchronizing EEG recording with EmotivPro and inserting event markers at stimulus onset. It also records behavioral response, including timestamps for stimulus onset and key presses, thus allowing for the calculations of response times.

4 Findings

4.1 Behavioral Response Time

Figure 4 presents participants' response times across five traffic scenarios. In the "Minimal Traffic Volume" scenario (M = 4.02s, 95% HDI [1.91s, 7.04s]), participants exhibited longer decision times and greater variability compared to the "Low Traffic Volume" scenario (M = 2.62 s, 95% HDI [2.07s, 4.76s]). The absence of clear traffic cues on an empty road seemed to lead to more diverse decision strategies and greater hesitation. On the other hand, the "High Traffic Volume" scenario (M = 8.08 s, 95% HDI [3.17s, 23.53s]) introduced dense traffic flow and significantly increased decision difficulty to identity a safe crossing gap. Some participants adopted a cautious, risk-averse approach, waiting longer for an ideal opening, while others navigated traffic more aggressively.

For intersection scenarios, in the "Surface-marked Intersection", the signalized turning vehicle introduced additional hesitation (M = 4.36 s, 95% HDI [1.79s, 9.73s]) compared to continuous vehicular flow (in "Low Traffic Volume"). This hesitation, as reported in retrospective think-aloud sessions, stemmed from the need to confirm whether the stopped vehicle would remain stationary behind the stop line and give pedestrian right-of-way. The added uncertainty increased evidence accumulation thresholds, aligning with predictions from the drift diffusion model (McIntosh & Sajda, 2020). In the "Signalized Intersection" scenario, participants took longer to respond (M = 5.27s, 95% HDI [2.23s, 14.59s], likely due to the need to process additional sensory cues—the traffic light. This suggests that decision-making in road-crossing did follow a sequential process, where participants first perceived and interpreted the environment, then conformed safety and prepared the motor, finally initiated movement.

Overall, these behavioral results indicated that participants were actively engaged in the tasks, and the five traffic scenarios successfully elicited a range of decision-making strategies. Simpler conditions encouraged fast, heuristic responses, while more complex scenarios required deliberative processing. Additionally, the results captured individual differences in risk tolerance, with some participants demonstrating aggressive, decisive behaviors, while others exhibited more conservative, risk-averse strategies, as reflected in their response times and variability.
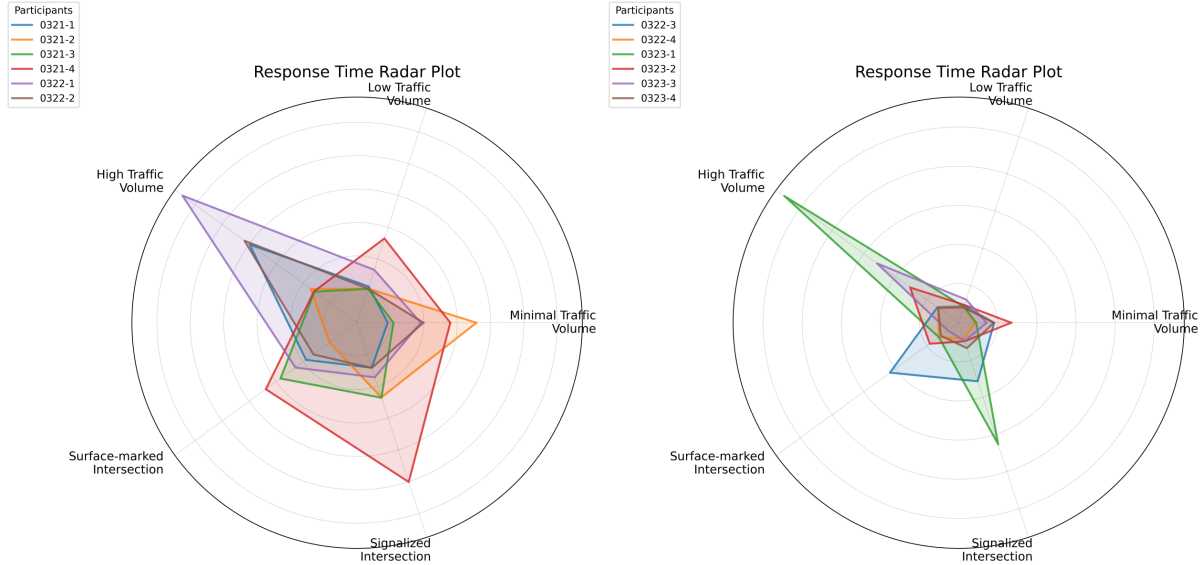
Figure 4. Radar plots of response time for all participants across the five traffic scenarios.

4.2 EEG Results

Figure 5 shows the butterfly plots (raw EEG signal traces over time) with scalp topographies (scalp distribution) of the event-related brain activities. Topographies were placed at timepoints that segmented the sequence into four time intervals. The response time in Figure 5(a) and Figure 5(b) is 2.145s and 2.845s, respectively. We observed strong positive activations (increase in amplitude) over left frontal electrodes emerging around 0.5s preceding the reach of the response action. Prior to this, the EEG topographies show low or negative frontal activation, indicating that the strong left frontal activity is built up leading up to the response reach/motor preparedness. This helps us pinpoint the localized spatial electrode, but it remains unclear which frequency band (and associated cognitive functions) modulated this motor planning and readiness.

Figure 6(a) shows the PSD across frequencies from 14 channels. The trend indicates a 1/f-like power decrease, where lower frequencies have higher power, while higher frequencies show a gradual drop in power. Figure 6(b) shows EEG power distribution across the scalp. Overall, we can observe stronger activation in the frontal regions. Based on the color scale values, theta and alpha power are notably stronger compared to higher frequency bands. Figure 6(c-e) further provides a time-resolved view of frequency power changes at electrode F4 with three spectral estimation methods. The Morlet FFT method demonstrates better time resolution compared with Multitaper, while Multitaper provides better frequency resolution. In addition, Figure 6(c) shows the power changes relative to the baseline mean, where power from only low frequency ranges (theta) is observed around 0.6s post-stimulus), whereas higher-frequency power seems to be filtered out. In contrast, Figure 6(d-e) indicate that log-transformed normalization retains higher-frequency components. According to Figure 6(e), where the Multitaper method provides a more stable power estimation, the dominant frequency bands are observed in theta and alpha during the earlier perception stage and high beta that remains sustained till the motor preparation and execution.
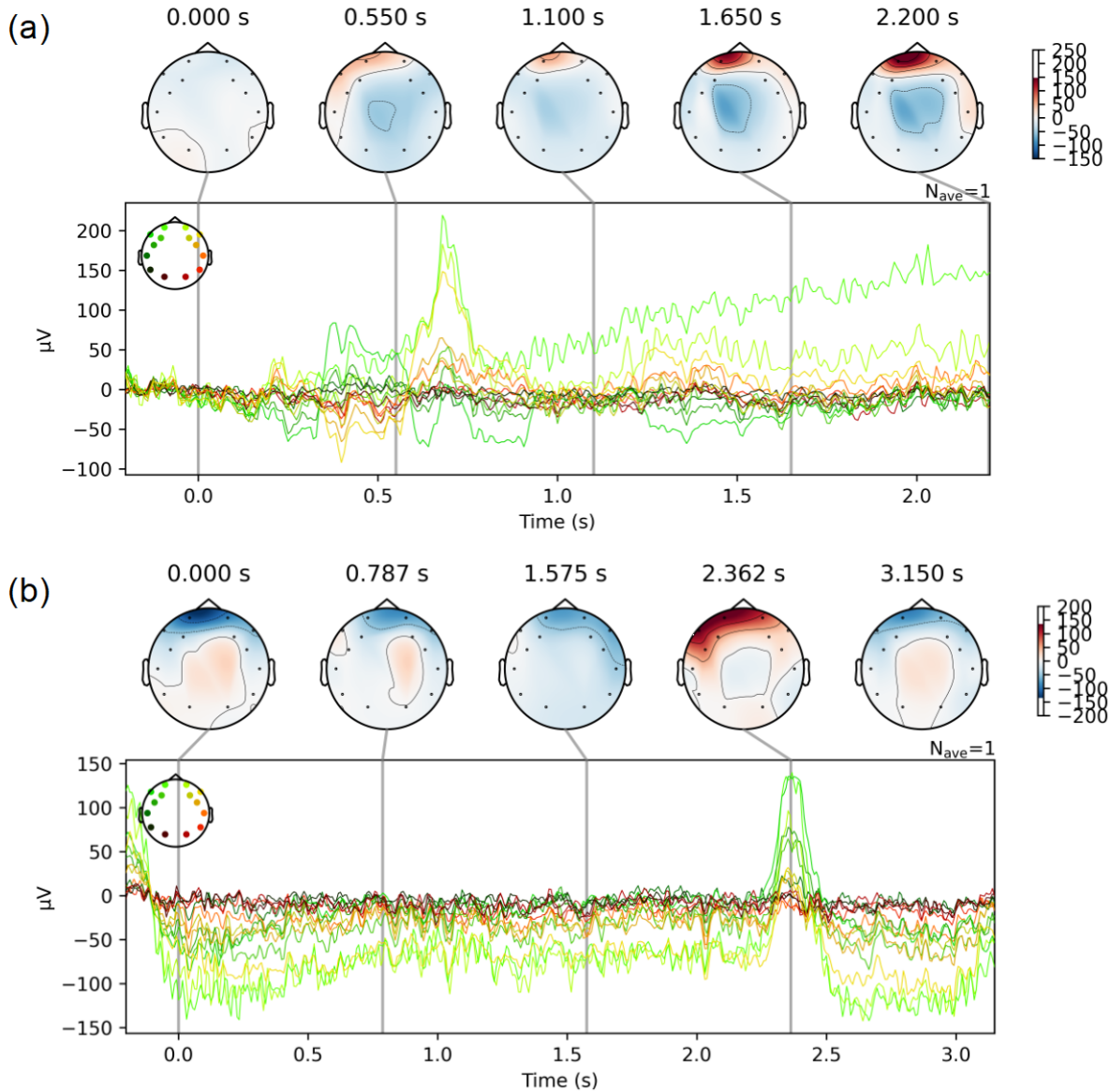
Figure 5. Joint plots combing butterfly plots with scalp topographies in (a) the "Low Traffic Volume" scenario and (b) the "Signalized Intersection" scenario.

Figure 7 provides an overview regarding oscillatory effects across both time and space. From the spatial differences in scalp topographies, it is clear that theta-band dominant oscillatory activity around 0.65s post-stimulus peak (presumably corresponding to the perception stage) is strongly frontal and left-lateralized, with suppression over parietal-temporal regions. This pattern is highly likely associated with theta-band activity modulated sensory processing and attentional control during perception (Karakaş, 2020). Later, the activation shifts to a strong high-beta band response in the frontocentral area, which is closely linked to motor areas that are committed to decision reach and motor readiness 2s-post stimulus (with reference to the 2.145s response time in this trial) (Wagner et al., 2017).
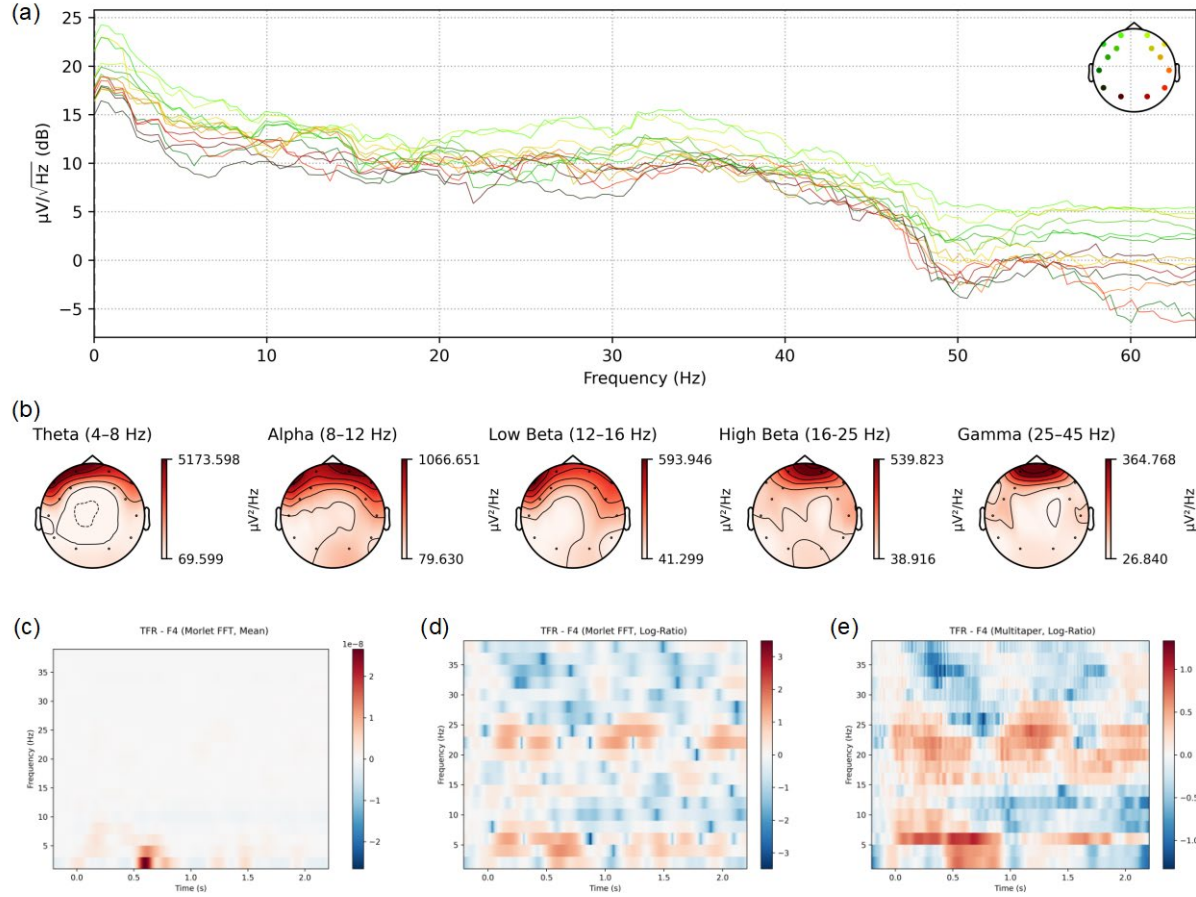
Figure 6. (a) Power Spectral Density across frequencies (0-65 Hz) over 14 EEG channels. (b) Interpolated scalp topography of power in five specific frequency bands. (c-e) Time-Frequency Representations (TFRs) at electrode F4 using Morlet FFT with a mean baseline correction, Morlet FFT with a log ratio baseline correction, and a Multitaper with a log ratio baseline correction method respectively.

Strong low-frequency frontal activity suggests top-down control during the perception stage (Helfrich et al., 2017). However, it remained unclear about the network dynamics and which posterior region the frontal area primarily modulates for guided visual perception and processing. From the functional connectivity analysis, we observed that at 0.812s post-stimulus in the evoked response, there was high theta phase coupling on a global scale (see Figure 8(a)). To investigate individual channel-level in more detail, we visualized the connectivity matrix and sensor connectivity at 0s pre-stimulus (Figure 8(c) and at the timepoint with most global theta connectivity after stimulus presentation (Figure 9(c)(g)). A hemispheric shift was observed during perception, with connectivity initially emerging between the left hemisphere and the right posterior regions (P8, O2). Later, stronger connectivity developed between the right frontal regions and the left posterior areas (P7, O1). This reorganization of neural circuits aligns with previous neurophysiological findings on hemispheric asymmetries that the right hemisphere is more specialized for spatial reasoning (Sun & Walsh, 2006).
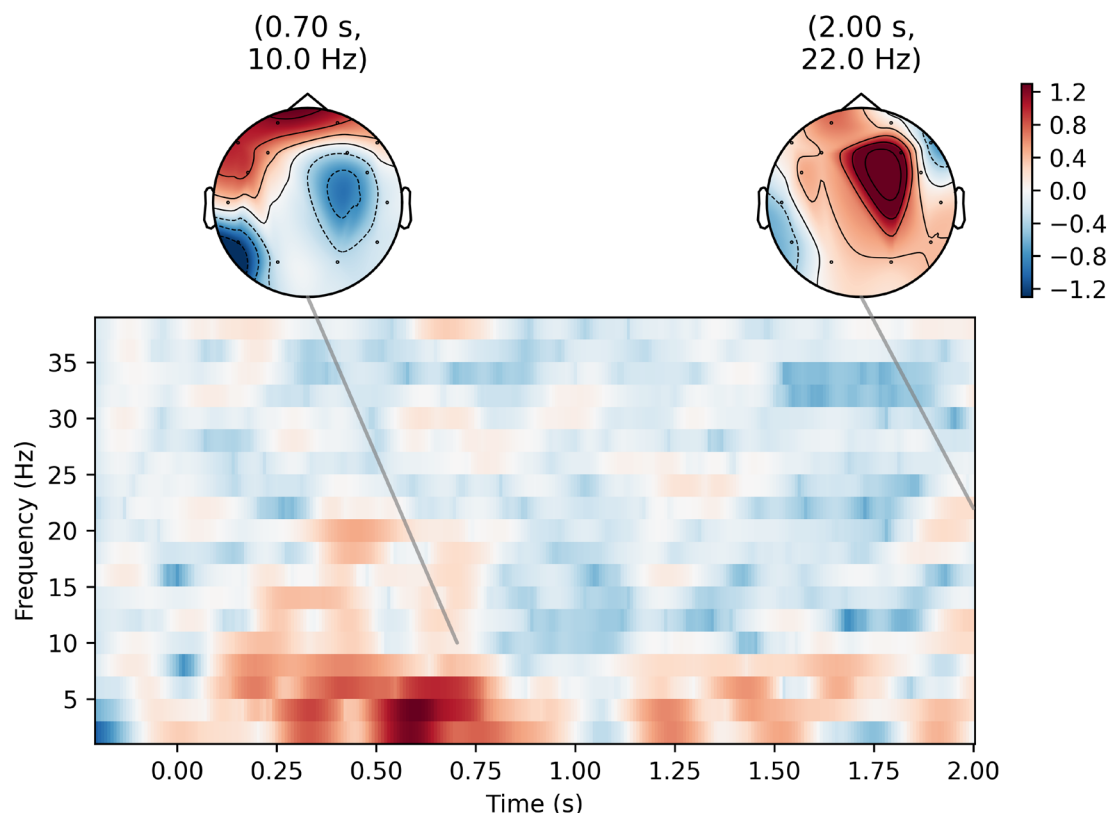
Figure 7. A joint plot showing the aggregated TFR across channels and topomaps at two specific times and frequencies.
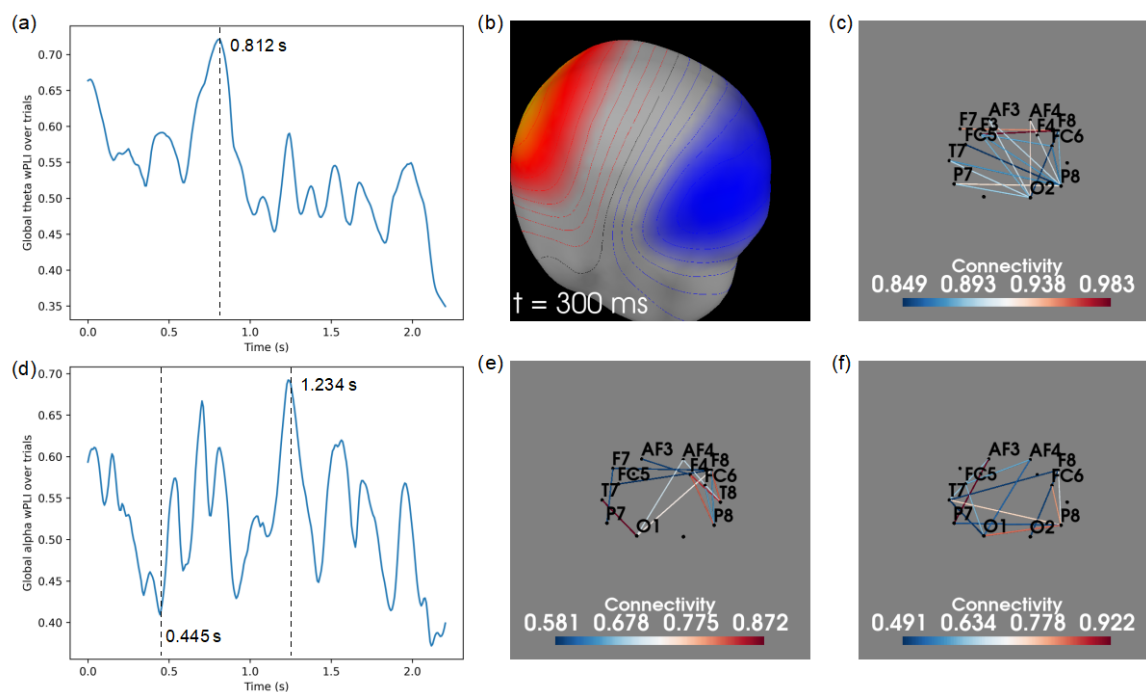

Figure 8. (a),(d) Global wPLI for theta and alpha bands. (b) 3D Field Map at 0.3s post-stimulus. (c),(e),(f) sensor connectivity for theta (0s pre-stimulus), alpha (0.445 post-stimulus), and high beta (0.055 post-stimulus).

The initial left frontal dominant connectivity is highly likely associated with the proactive inhibitory control mechanism that started before stimulus onset and was released concomitantly to the stimulus appearance (Sulpizio et al., 2017). The hemispheric shift suggests a cross-hemispheric complementary frontal mechanism under perceptual uncertainty (Tsumura et al., 2021). Although this functional connectivity analysis does not provide direction information, previous findings from effective connectivity studies indicate that frontal-to-posterior connectivity is dominant when the stimulus is ambiguous, whereas posterior-to-frontal connectivity emerges when the stimulus information is more distinctive (Tsumura et al., 2021). Given that the left frontal region was more activated but connectivity later shifted to a right frontal–left posterior pattern, we speculate that proactive inhibitory control, a top-down process dominated by the left frontal region, played a key role in early perception. However, this was supplemented by bottom-up stimulus-driven sensory processing, facilitated by the right frontal region. This interpretation appears logical because around 0.8s post-stimulus, the vehicle first appears in view in this low-traffic scenario, which evidently necessitates bottom-up processing to assess the environment.
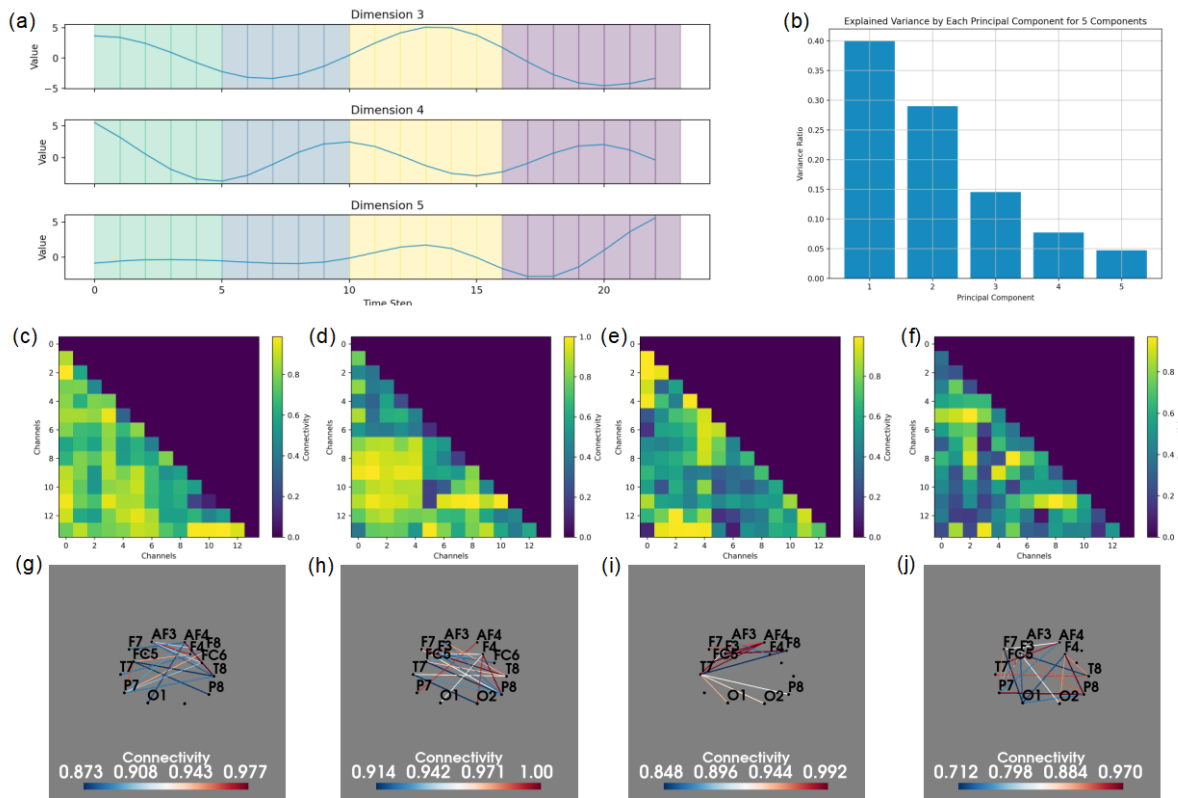
Figure 9. (a) Durations of cognitive microstates decomposed by HMM from representation principal components. (b) Explained variance by the top 5 principal components from PCA. (c)-(f) Sensor connectivity matrices for theta (0812s post0stimulus), alpha (1.234s post-stimulus), alpha (2s post-stimulus, high-beta (2s post-stimulus.) (g)-(j) Corresponding connectivity visualizations for the above matrices.

In the alpha-band connectivity from the lowest global wPLI timepoint (0.445s) (Figure 8(e) to the global wPLI peak (1.234s) (Figure 9(h)) and to 2s post-stimulus (Figure 9(i)), we observed clear alpha suppression during the early perception stage that indicates active sensory processing for visual encoding (e.g., to detect a stimulus). Later, when more task-relevant visual cues became available, alpha-band connectivity increased globally for inhibitory control to actively gate irrelevant sensory input. As participants transitioned from perception to action, alpha modulation localized to the frontal area to mediate action execution (Filippi et al., 2020).

For high-beta modulations, comparing the lowest global high-beta wPLI at 0.055s after stimulus (Figure 8(f) with the connectivity patterns at timepoint 2s post stimulus (Figure 9(j)), we observe a clear transition in network configurations. Specifically, the motor area, reflected in the nearest channel F4, was completely absent from the activation network during the perception stage (as shown in Figure 8(f)). However, as the brain transitions into motor preparedness, strong activation emerges in F4, along with increased connectivity between F4 and P8. This pattern aligns with findings from mammalian studies, which have identified a sensorimotor cortical network where the motor cortex connects to the posterior parietal cortex to support goal-directed actions (Martínez-Vázquez & Gail, 2018).

Overall, these neurophysiological signatures provide insights into how the brain flexibly reconfigures cognitive resources during the perception-action transitions for decision-making and motor planning.

4.3 Latent Microstates Mediating Perception-Action Decomposed by HMM

The above results reveal clear neural patterns, but to develop a computational method that quantitively establishes the predictive window for motor preparedness, we constructed the HMM to decompose the EEG sequences to four microstates. Temporal markers differentiating these microstates were used to segment and isolate distinct cognitive stages, and statistical analysis was performed to identify the PSD feature that best distinguishes stage transitions. Subsequently, we constructed a machine learning technique with a sliding window to predict the moment of motor readiness and investigated the lookahead time window that yields optimal prediction performance.

First, the 70-dimension EEG data were standardized by removing the mean and scaling to unit variance to account for sequence variance. The standardized data were then submitted to Principal Component Analysis (PCA) (Yu et al., 2014) to compress the feature space. The top five principal components and their explained variance are shown in Figure 9(b), which cumulatively preserved approximately 94% of the variance. Subsequently, the constructed Gaussian HMM was applied to the principal components on a trial basis, and model convergence was tracked. If the model converged, microstates were predicted based on the posterior probabilities and then sorted in order. Figure 9(a) demonstrates the temporal structure and four microstate transitions over time (with shaded areas showing the duration of each cognitive microstate). The temporal markers that differentiated the microstates were then used to segment each sequence into four microstates on a trial basis and labeled for all participants. Later, the 25th (Q1) and 75th (Q3) percentiles of each segment were calculated as the Interquartile Range (IQR). Data points outside the range Q1 - 1.5 × IQR and Q3 + 1.5 × IQR were classified as outliers and excluded from the subsequent analysis.

Since PSD data distributions characterized by each EEG microstate from multi-channels did not fit a normal distribution (*p* value>0.05 based on Shapiro-Wilk test), Friedman's Analysis of variance (ANOVA)—a non-parametric alternative to repeated measures ANOVA—was used to analyze differences across the four cognitive microstates to improve statistical robustness (Friedman, 1937). Following a significant result in Friedman's ANOVA, Conover's post-hoc tests were conducted to identify specific pairwise differences between microstates. All statistical tests were two-tailed, with the null hypothesis assuming no significant difference in mean values across subgroups using a 5% significance level. While p-values determined whether statistically significant differences existed between subgroups, t-scores provided information on the magnitude and the direction of differences, and Cohen's *d* quantified the effect size, indicating the strength of the observed differences. Figure 10 highlights the feature dimensions with significant results, which were pronounced in frontal areas.
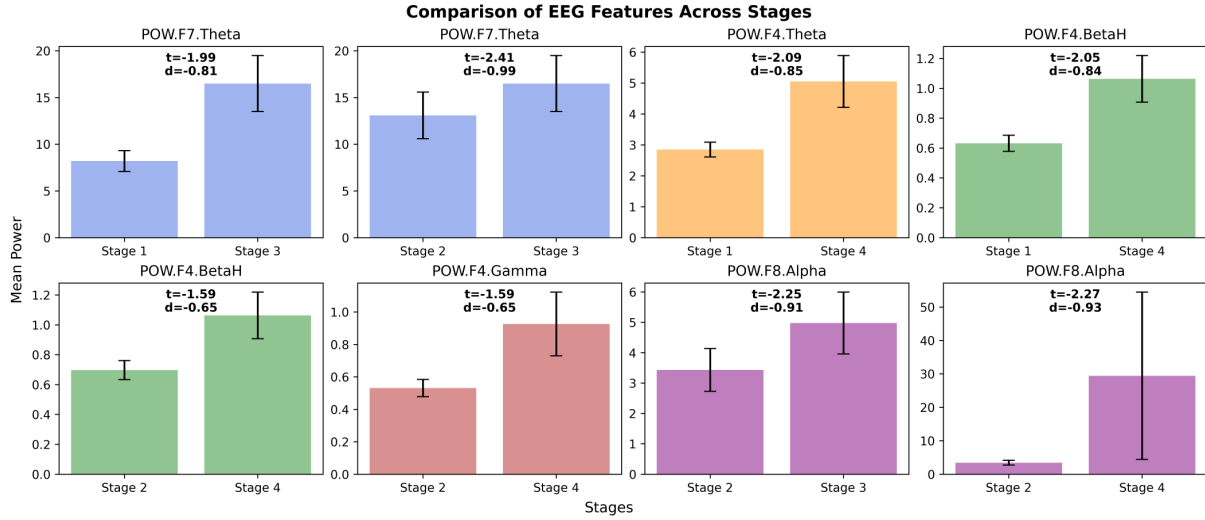
Figure 10. Post-hoc comparisons and significant results with the t-value and Cohen's d. The bars represent the standard deviation. Colors differentiate the features.

Except for theta-band at the left frontal region (F7) with its established role in initial perceptual processing (Karakaş, 2020), we also observed alpha-band ERD at the right frontal region (F8) that complements attentional inhibition to selectively isolate critical environmental cues for sensory processing (Foxe & Snyder, 2011). These neurophysiology signatures suggest a hierarchical perpetual mechanism, where the brain first engages in broad perceptual surveillance of the environment and then shifts to a more focused assessment of critical cues to drive evidence accumulation for decision-making.

Transitioning to the action stage, consistent with scalp topographies from the TFR, we observed significantly stronger high-beta oscillations in the right-frontal region (F4). This finding aligns with right frontal beta-band's established role in motor planning (Wagner et al., 2017). Additionally, this process was supplemented by higher-frequency (gamma) band activity that mediates high-order cognitive control for decision resolution and response execution preparation (Jensen et al., 2007; Polanía et al., 2012).

4.4 Classification Performance for Predicting Road-Crossing Initiation

The above results demonstrate that before the physical execution of a motor response, there is preparatory neural activity mediated by high-beta oscillations in the right frontocentral area (F4). Using data from this feature dimension, a comparative analysis was conducted to evaluate all possible combinations of sliding window length and stride and their impact on classifier performance. For example, with a sliding window of 9 data points (1.125s, give the 8Hz sampling rate) and a stride of 3 data points (0.375s), we obtained 838 segments for training the classifier and achieved 80% accuracy. As window length and stride increased, the dataset size decreased. For instance, with a sliding window of 11 data points (1.375s) and a stride of 7 data points (0.875s), the dataset was reduced to 356 segments, but accuracy increased to 83%.

Given the variability in dataset size, Receiver Operating Characteristic (ROC) curves were generated to evaluate the classifier's discriminative ability at various levels of sensitivity and specificity. The Area Under the Curve (AUC) was used as the performance metric, where a higher AUC indicates a better trade-off between True Positive Rate and False Positive Rate across different classification thresholds. The results showed that a sliding window of 1.125s with a stride of 0.375s yielded an AUC as high as 0.91 (see Figure 11(a)). To assess whether this performance was due to chance, we applied the same sliding window configuration and future dimension in a permutation test, where segment labels were randomly shuffled and submitted to five-fold cross validation. The AUC dropped from 0.91 to 0.52 (see Figure 11(b)),which corresponds to chance level for binary classification. This confirms that the classifier's strong performance was not merely the result of random chance.
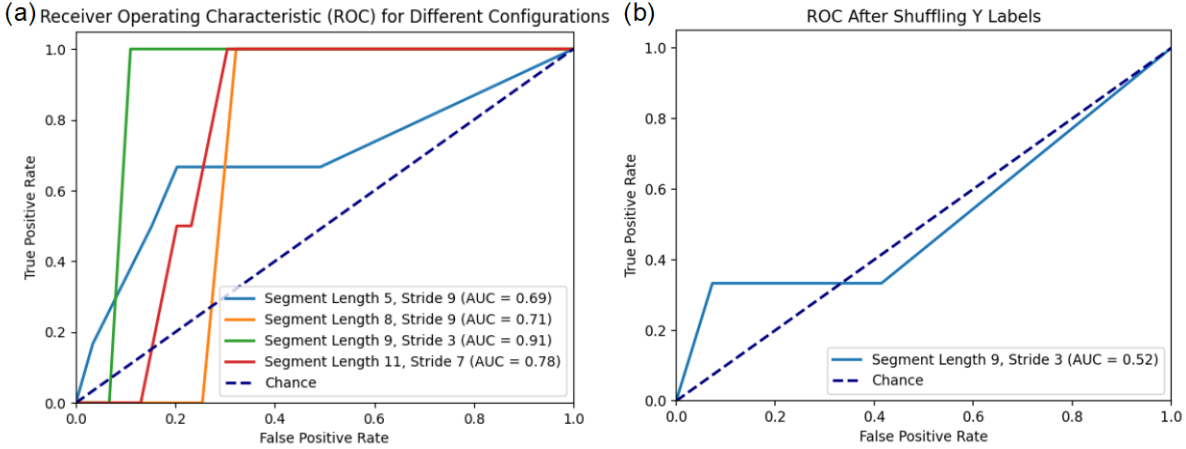
Figure 11. (a) ROC curves and AUC for representative sliding window configurations. (b) ROC curves for the chosen sliding window and the chance level.

5 Recommendations

5.1 Brain Dynamics in Embodied Perception and Motor Planning

Neuroimaging studies have provided extensive evidence on motor readiness, but no computational approach using machine learning techniques has been developed to predict motor readiness for real-world applications. This study introduces a new framework that, when applied to high temporal resolution EEG signals, can predict imminent motor actions preceding physical execution. This advancement opens new possibilities for EEG applications, extending beyond its traditional role as an ergonomic tool for stress and fatigue monitoring to motor planning in human-robot interactions. In this work, we evaluate the framework for intelligent transportation systems, demonstrating the potential for communication of motor intentions in VRUs' road-crossing behaviors with AVs. This could be particularly beneficial in scenarios where VRUs are in AVs' blind spots, beyond the reach of traditional onboard sensors, or in situations involving ambiguous behaviors such as jaywalking. Beyond transportation, this technical framework is highly adaptable to other motor behaviors, such as handover coordination in industrial and assistive robot collaboration. Therefore, we believe this work offers promise to expand the horizon of neurodevices and facilitate seamless human-robot interaction in diverse real-world applications.

In addition, this work introduces new strategies for studying brain mechanisms underlying complex decision-making tasks, particularly those structured as a perception-action loop. We applied HMMs to decompose EEG microstates and examined dynamic functional connectivity across different frequency components, revealing how cluster activation and neural circuits shift between perception and action. This study is among the first EEG-based investigations to model microstate transitions in real-life, visually guided perception and motor planning. In contrast, most existing EEG approaches assume stationary cognitive states or consider only very slow state transitions. To further account for variability in temporal dynamics, our classifier integrates the DTW technique that adapts to differences in interval durations across microstates when making predications based on multivariant EEG signals.

5.2 Practical Implications in "Cognitive Internet of Road Agents"

By empowering VRUs as active beacons of their immediate road-crossing behaviors, this approach holds the potential to reshape the next generation of Vehicle-to-Everything (V2X) communication, emphasizing a cognitive layer of processing (Chen et al., 2018). In this vision, every road agent—whether a vehicle, VRU, or infrastructure element—functions as a smart, interconnected node within a larger network of shared information (Yang et al., 2022). Here, the flow of information is not merely mechanistic but enhanced through signal processing, enabling an adaptive and intelligent response system. At the core of this network, predictive models of pedestrian behavior serve as a foundation for automated, context-aware interactions with AVs, for safer and efficient human-vehicle collaboration in dynamic traffic environments.

5.3 Methodological Strengths and Limitations

Our framework, built upon high temporal resolution EEG signals, offers a new direction for studying dynamic characteristics in motor planning. By integrating neurophysiological sensing with advanced signal analysis techniques—including time-frequency analysis, functional connectivity, and microstate decomposition—this approach provides fine-grained insights into cognitive processes that traditional retrospective self-reported methods (such as surveys or interviews in "thinking aloud" studies) cannot capture at the same level of detail. Secondly, higher-order cognitive functions are embedded in time-varying neural activities and network dynamics, which cannot be effectively measured using other physiological sensors such as heart rate or galvanic skin response (GSR) (Yi et al., 2023). More importantly, neural modulations can serve as predictive markers—supporting proactive expectation mechanisms in perception and mediating action execution.

This is the first "anticipatory" study that brings the notion of lead time into perspective. This provides a key advantage over previous reactive sensing methods, as in high-speed environments—for instance, for a car travelling at 25-45 mph—even a one-second anticipation time can provide significantly increased braking time and distance, thereby lowering the risk and impact of collisions. Before autonomous vehicles becomes predominant, the proposed system also brings practical significance in the human-supervisory stage by reminding human drivers to stay focused in preparation for emergency takeovers in such alerted pedestrian crossing situations. These advancements are made possible by the proposed improvements in computational neuroscience. Our approach leverages probabilistic reasoning based on statistical dependencies to segment cognitive microstates and effectively accounting for temporal variability (phase lags across trials) in non-structured (self-paced) decision-making tasks. This moves beyond traditional structured design of psychology experiments and the reliance on expert-defined epoching for dataset preparation when employing machine learning techniques.

This study provides a proof-of-concept for a computational neuroscience approach to predicting motor preparedness. However, the findings are derived from a modest sample size (12 participants with balanced gender). The current results need to be generalized with a larger appropriate sample size in subsequent studies and validated in a controlled real-world testing field, such as the Mcity Testing Facility (Mcity). The dataset in this study was designed with variability introduced by environmental cues and interactions in five traffic scenarios and different participant behaviors (as reflected in behavioral response time). This range aimed to prevent overfitting of the machine learning classifier in homogenous trials settings and to improve the model's generatability to real-world applications. However, it would not be surprising if inter-individual variability existed. For instance, some participants may exhibit more conservative behaviors, while others may be more aggressive.

In addition, the differences in decision-making strategies across different traffic scenarios were expected, with simpler situations eliciting intuitive/heuristic decision-making, while hesitation or caution are demonstrated in more complex environments, or even introducing rolling gap behaviors in multi-lane settings (Zafri et al., 2022). Urgency can affect individuals' decision thresholds, emotional arousal and sensorimotor processing (Steinemann et al., 2018). Despite these heterogeneities, we assume that the cognitive microstate transitions are repeatable in all situations and across individuals, and we account for the temporal distortions in microstate time course when constructing the classifier. However, the potential demographic differences in pedestrian behaviors and the interaction patterns with traffic infrastructure and AVs in different speed, vehicular density, and external Human-Machine Interfaces lead to our future studies that would be directed toward understanding the differences in neural dynamics and cognitive processes, and thus design targeted traffic policies and safety intervention programs for safer, and more efficient traffic systems in the AV coexistence era.

6 Impacts

This project explored the predictive capabilities of EEG signals for predicting pedestrian road-crossing initiation, situated within the broader context of V2X communications, specifically Vehicle-to-Pedestrian (V2P) dynamics. The researched approach addresses the gaps in vision-based methods, such as dynamic

modeling of positional data and skeletal analysis, particularly when pedestrians are occluded and motionless but may initiate abrupt actions unpredictably. First, the HMM provided a detailed quantitative analysis of the temporal progression in cognitive microstates. Further statistical analysis aligned with the findings from neural activation and brain connectivity about brain dynamics and pinpointed frontal theta and alpha oscillations modulating early perceptions, while high-beta in the frontocentral area modulating later motor action preparation and execution. Finally, the constructed KNN classifier, augmented with the DTW distance metric and optimized sliding window configurations, provided an AUC of 0.91 based on frontocentral cortex activities, with an approximate 1-second anticipatory lead window, for predicting pedestrian road-crossing initiation.

The developed method empowers pedestrians as active beacons for automatically broadcasting their road-crossing initiation, marking a significant stride towards the realization of a fully connected and cognitive ecosystem of road agents. The technical framework is also adaptable to a wide range of human-vehicle interaction scenarios that involve motor planning and readiness. For example, it can be applied to bicycle-vehicle interactions, where a CAV must anticipate and coordinate with bicyclist intent and movement to ensure a smooth and timely resolution of interactions. Similarly, it can enhance assistive robotic systems in traffic, such as smart mobility wheelchairs, by enabling them to predict human intentions and adjust speed and trajectory accordingly for seamless coexistence in traffic.

7 Research Products

The work on this project has produced the following products:

U.S. Serial No. 63/810,537, "*Method to Use EEG Signals to Determine VRU Intent in V2X Traffic Architectures*," [**Patent Application**] filed with the U.S. Patent and Trademark Office and assigned to UM, May 2025.

Zhou, X., Menassa, C., and Kamat, V. (2025). A Wearable EEG Dataset for Road Crossing Decision-Making [**supporting dataset**]. https://doi.org/10.7302/1a78-9t04

Zhou, X., Menassa, C. C., & Kamat, V. R. (2025). Siamese network with dual attention for EEG-Driven social Learning: Bridging the Human-Robot gap in Long-Tail autonomous driving. Expert Systems with Applications, 128470. https://doi.org/10.1016/j.eswa.2025.128470

Zhou, X., Menassa, C. C., & Kamat, V. R. (2025). Hands-Free Crowdsensing of Accessibility Barriers in Sidewalk Infrastructure: A Brain–Computer Interface Approach. Journal of Infrastructure Systems, 31(2), 04025008. https://doi.org/10.1061/JITSE4.ISENG-2620

Zhou, X., Menassa, C. M., & Kamat, V. R. (2025). Towards Probabilistic Inference of Human Motor Intentions by Assistive Mobile Robots Controlled via a Brain-Computer Interface. arXiv preprint arXiv:2501.05610. https://arxiv.org/abs/2501.05610

Zhou, X., Menassa, C. M., & Kamat, V. R. (2025). Biologically Inspired Predictive Coding TCN-Transformer for Anticipatory Human-Robot Interaction in Shared Physical Spaces. arXiv preprint arXiv:2405.13955. https://arxiv.org/abs/2404.03498

COVERT: Cognitive Internet of Vulnerable Road Users in Traffic

Outputs:

- U.S. Serial No. 63/810,537, "*Method to Use EEG Signals to Determine VRU Intent in V2X Traffic Architectures*," [**Patent Application**] filed with the U.S. Patent and Trademark Office and assigned to UM, May 2025.

- Zhou, X., Menassa, C., and Kamat, V. (2025). *A Wearable EEG Dataset for Road Crossing Decision-Making* [**Supporting Dataset**]. https://doi.org/10.7302/1a78-9t04

- Zhou, X., Menassa, C. C., & Kamat, V. R. (2025). *Siamese network with dual attention for EEG-Driven social Learning: Bridging the Human-Robot gap in Long-Tail autonomous driving*. Expert Systems with Applications, 128470. https://doi.org/10.1016/j.eswa.2025.128470

- Zhou, X., Menassa, C. C., & Kamat, V. R. (2025). *Hands-Free Crowdsensing of Accessibility Barriers in Sidewalk Infrastructure: A Brain–Computer Interface Approach*. Journal of Infrastructure Systems, 31(2), 04025008. https://doi.org/10.1061/JITSE4.ISENG-2620

- Zhou, X., Menassa, C. M., & Kamat, V. R. (2025). *Towards Probabilistic Inference of Human Motor Intentions by Assistive Mobile Robots Controlled via a Brain-Computer Interface*. arXiv preprint arXiv:2501.05610. https://arxiv.org/abs/2501.05610

- Zhou, X., Menassa, C. M., & Kamat, V. R. (2025). *Biologically Inspired Predictive Coding TCN-Transformer for Anticipatory Human-Robot Interaction in Shared Physical Spaces*. arXiv preprint arXiv:2405.13955. https://arxiv.org/abs/2404.03498

COVERT: Cognitive Internet of Vulnerable Road Users in Traffic

Outcomes

The results of our technical experiments showed that theta oscillatory power in the frontal lobe achieved an Area Under the Curve of 0.91 in predicting a pedestrian's intended road crossing, with approximately a 1-second lead window before any physical movement occurred. These promising results signify a transformative shift towards pedestrians proactively and automatically signaling their intended behavior and trajectories, rather than being passively and reactively sensed by external sensors, enabling forward-thinking and adaptive vehicle-to-everything (V2X) architectures for enhanced safety and mobility.

Brain Dynamics in Embodied Perception and Motor Planning: Neuroimaging studies have provided extensive evidence on motor readiness, but no computational approach using machine learning techniques had been developed to predict motor readiness for real-world applications. This project introduced a new framework that, when applied to high temporal resolution EEG signals, can predict imminent motor actions preceding physical execution. This advancement opens new possibilities for EEG applications, extending beyond its traditional role as an ergonomic tool for stress and fatigue monitoring to motor planning in human-CAV interactions. We evaluated the framework for ITS, demonstrating the promise of anticipatory communication of motor intentions in VRUs' road-crossing behaviors with CAVs.

Practical Implications in "Cognitive Internet of Road Agents": By empowering VRUs as active beacons of their immediate road-crossing behaviors, this approach holds the potential to reshape the next generation of Vehicle-to-Everything (V2X) communication, emphasizing a cognitive layer of processing. In this, every road agent—whether a vehicle, VRU, or infrastructure element—functions as a smart, interconnected node within a larger network of shared information. Here, the flow of information is not merely mechanistic but enhanced through signal processing, enabling an adaptive and intelligent response system. At the core of this network, predictive models of pedestrian behavior serve as a foundation for automated, context-aware interactions with AVs, facilitating safer and more efficient human-vehicle collaboration in dynamic traffic environments.

The following patent application was filed during this performance period

U.S. Serial No. 63/810,537, "*Method to Use EEG Signals to Determine VRU Intent in V2X Traffic Architectures*," Patent application filed with the U.S. Patent and Trademark Office and assigned to UM, May 2025.

The primary innovation described and claimed is a computing system for analyzing electrophysiological signals obtained from a vulnerable road user to predict a road usage intent prior to physical motion includes: a processor and a memory having stored thereon computer-executable instructions that, when executed, cause the computing system to (1) receive electroencephalogram signals from a vulnerable road user; (2) preprocess the received signals to extract temporal and spectral features indicative of cognitive state transitions; (3) apply a Hidden Markov Model to identify cognitive state transitions associated with road usage decisions; and (4) generate a prediction of road usage behavior based on the identified cognitive state transitions.

In summary, this project developed the predictive capabilities of EEG signals for predicting pedestrian road-crossing initiation, situated within the broader context of V2X communications, specifically Vehicle-to-Pedestrian (V2P) dynamics.

COVERT: Cognitive Internet of Vulnerable Road Users in Traffic
Impacts

This project has developed and tested the feasibility of new methods that allow VRUs' road usage intentions to be interpreted in real-time using wearable biosensing and advanced machine learning algorithms. This approach leverages humans 'inherent cognitive capacities as sensors and has the potential to be more reliable and widely deployable compared to existing methods that rely on cooperative sensing of CAVs in forecasting VRUs' future motion trajectories. Integration of the developed methods into V2X architectures promises to improve road safety, enhance traffic flow, and increase societal trust and acceptance of CAVs.

The developed method and computational framework, built upon high temporal resolution EEG signals, offers a new direction for studying dynamic characteristics in motor planning. By integrating neurophysiological sensing with advanced signal analysis techniques—including time-frequency analysis, functional connectivity, and microstate decomposition—this approach provides fine-grained insights into cognitive processes that traditional retrospective self-reported methods cannot capture at the same level of detail. Secondly, higher-order cognitive functions are embedded in time-varying neural activities and network dynamics, which cannot be effectively measured using other physiological sensors such as heart rate or galvanic skin response (GSR). More importantly, neural modulations can serve as predictive markers—supporting proactive expectation mechanisms in perception and mediating action execution.

This project was the first "anticipatory" study that brings the notion of lead time and VRU motion intent prediction into perspective. This provides a key advantage over previous reactive sensing methods, as in high-speed environments—for instance, for a car travelling at 25-45 mph—even a one-second anticipation time can provide significantly increased braking time and distance, thereby lowering the risk and impact of collisions. The project team took decisive steps to bring the developed research outcomes into commercialization practice. This has been done through patent filing developing a research partnership with HATCI. This will allow future research to develop a POC for demonstration of practicality.

The work on this project has produced the following products:

- U.S. Serial No. 63/810,537, "*Method to Use EEG Signals to Determine VRU Intent in V2X Traffic Architectures*," [**Patent Application**] filed with the U.S. Patent and Trademark Office and assigned to UM, May 2025.
- Zhou, X., Menassa, C., and Kamat, V. (2025). *A Wearable EEG Dataset for Road Crossing Decision-Making* [**Supporting Dataset**]. https://doi.org/10.7302/1a78-9t04
- Zhou, X., Menassa, C. C., & Kamat, V. R. (2025). *Siamese network with dual attention for EEG-Driven social Learning: Bridging the Human-Robot gap in Long-Tail autonomous driving*. Expert Systems with Applications, 128470. https://doi.org/10.1016/j.eswa.2025.128470
- Zhou, X., Menassa, C. C., & Kamat, V. R. (2025). *Hands-Free Crowdsensing of Accessibility Barriers in Sidewalk Infrastructure: A Brain–Computer Interface Approach*. Journal of Infrastructure Systems, 31(2), 04025008. https://doi.org/10.1061/JITSE4.ISENG-2620
- Zhou, X., Menassa, C. M., & Kamat, V. R. (2025). *Towards Probabilistic Inference of Human Motor Intentions by Assistive Mobile Robots Controlled via a Brain-Computer Interface*. arXiv preprint arXiv:2501.05610. https://arxiv.org/abs/2501.05610
- Zhou, X., Menassa, C. M., & Kamat, V. R. (2025). *Biologically Inspired Predictive Coding TCN-Transformer for Anticipatory Human-Robot Interaction in Shared Physical Spaces*. arXiv preprint arXiv:2405.13955. https://arxiv.org/abs/2404.03498

References

Abiri, R., Borhani, S., Sellers, E. W., Jiang, Y., & Zhao, X. (2019). A comprehensive review of EEG-based brain-computer interface paradigms. *J Neural Eng, 16*(1), 011001.

Adobe. (2023). Creating a Motion tween animation. Retrieved from https://helpx.adobe.com/animate/using/creating_a_motion_tween_animation.html

Alahi, A., Goel, K., Ramanathan, V., Robicquet, A., Fei-Fei, L., & Savarese, S. (2016). *Social LSTM: Human Trajectory Prediction in Crowded Spaces*. Paper presented at the IEEE Conference on Computer Vision and Pattern Recognition (CVPR).

Almodfer, R., Fang, Z., Kong, X., & Zheng, S. (2015). Quantitative analysis of lane-based pedestrian-vehicle conflict at a non-signalized marked crosswalk. *Transportation Research Part F Traffic Psychology and Behaviour, 42*.

Alver, Y., & Katanalp, B. Y. (2022). Evaluating the Pedestrian Gap Acceptance in Semicontrolled Midblock Crosswalks with an Integrated AHP-FL Approach. *Journal of Transportation Engineering, Part A: Systems, 148*(9), 04022066.

Anaya, J., Merdrignac, P., Shagdar, O., & Nashashibi, F. (2014). *Vehicle to Pedestrian Communications for Protection of Vulnerable road Users*. Paper presented at the IEEE Intelligent Vehicles Symposium (IV).

Andreone, L., Guarise, A., Lilli, F., Gavrila, D., & Pieve, M. (2006). Cooperative Systems for Vulnerable Road Users: The Concept of the WATCH-OVER Project.

Anwar, D., Gupta, A., Naik, V., & Sharma, S. K. (2017, 4-8 Jan. 2017). *Detecting meditation using a dry mono-electrode EEG sensor*. Paper presented at the 2017 9th International Conference on Communication Systems and Networks (COMSNETS).

Arena, F., Pau, G., & Severino, A. (2019). V2X Communications Applied to Safety of Pedestrians and Vehicles. *Journal of Sensor and Actuator Networks, 9*, 3.

Bandyopadhyay, T., Jie, C., Hsu, D., Ang, M., Rus, D., & Frazzoli, E. (2013). *Intention-Aware Pedestrian Avoidance*: Experimental Robotics.

Bidgoly, A. J., Bidgoly, H. J., & Arezoumand, Z. (2022). Towards a universal and privacy preserving EEG-based authentication system. *Scientific Reports, 12*(1), 2531.

Bressler, S., Tang, W., Sylvester, C., Shulman, G., & Corbetta, M. (2008). Top-Down Control of Human Visual Cortex by Frontal and Parietal Cortex in Anticipatory Visual Spatial Attention. *The Journal of neuroscience : the official journal of the Society for Neuroscience, 28*, 10056-10061.

Brysbaert, M. (2019). How many participants do we have to include in properly powered experiments? A tutorial of power analysis with reference tables. *Journal of Cognition*.

Bunge, S. A. (2005). How we use rules to select actions: a review of evidence from cognitive neuroscience. *Cognitive, affective & behavioral neuroscience, 4*, 564-579.

Chauhan, H., Pakbaz, A., Jang, Y., & Jeong, I. (2024). Analyzing Trust Dynamics in Human–Robot Collaboration through Psychophysiological Responses in an Immersive Virtual Construction Environment. *Journal of Computing in Civil Engineering, 38*(4), 04024017.

Chavhan, S., Kumar, S., Gupta, D., Alkhayyat, A., Khanna, A., & Manikandan, R. (2023). Edge-Empowered Communication-Based Vehicle and Pedestrian Trajectory Perception System for Smart Cities. *IEEE Internet of Things Journal*.

Chayer, C., & Freedman, M. (2001). Frontal lobe functions. *Current neurology and neuroscience reports, 1*(6), 547-552.

Chen, J., Song, X., & Lin, Z. (2016). Revealing the "Invisible Gorilla" in construction: Estimating construction safety through mental workload assessment. *Automation in Construction, 63*, 173-183.

Chen, M., Tian, Y., Fortino, G., Zhang, J., & Humar, I. (2018). Cognitive Internet of Vehicles. *Computer Communications, 120*, 58-70.

Cheng, B., Fan, C., Fu, H., Huang, J., Chen, H., & Luo, X. (2022). Measuring and Computing Cognitive Statuses of Construction Workers Based on Electroencephalogram: A Critical Review. *IEEE Transactions on Computational Social Systems, 9*(6), 1644-1659.

Cochran, W., Cooley, J., Favin, D., Helms, H., Kaenel, R., Lang, W., Jr, G. C., Nelson, D., Rader, C., & Welch, P. (1967). What is the fast Fourier transform? *Proceedings of the IEEE, 15*, 1664-1674.

Cui, X., Wu, Y., Wu, J., You, Z., Xiahou, J., & Ouyang, M. (2022). A review: Music-emotion recognition and analysis based on EEG signals. *Front Neuroinform, 16*, 997282.

Datta, T., Jain, S., & Gruteser, M. (2014). *Towards City-Scale Smartphone Sensing of Potentially Unsafe Pedestrian Movements*. Paper presented at the IEEE 11th International Conference on Mobile Ad Hoc and Sensor Systems (MASS).

Deshmukh, A., Wang, Z., Guo, H., Ammar, D., Sherony, R., Feng, F., Lin, B., Bao, S., & Zhou, F. (2023). A Systematic Review of Challenging Scenarios Involving Automated Vehicles and Vulnerable Road Users. *Proceedings of the Human Factors and Ergonomics Society Annual Meeting, 67*.

Ding, L., & Gold, J. I. (2011). Neural Correlates of Perceptual Decision Making before, during, and after Decision Commitment in Monkey Frontal Eye Field. *Cerebral Cortex, 22*(5), 1052-1067.

Dong, W., Liu, Y., Zhu, W., Sun, J., & Bai, R. (2023). Temporal trends in the incidence and mortality of road injuries in China: Current trends and future predictions. *Injury, 54*(12), 111139.

Donner, T. H., Siegel, M., Fries, P., & Engel, A. K. (2009). Buildup of Choice-Predictive Activity in Human Motor Cortex during Perceptual Decision Making. *Current Biology, 19*(18), 1581-1585.

EMOTIV. (2023). EmotivPRO v3.0. Retrieved from https://emotiv.gitbook.io/emotivpro-v3/data-streams/frequency-bands

Eoh, H. J., Chung, M. K., & Kim, S. (2005). Electroencephalographic study of drowsiness in simulated driving with sleep deprivation. *International Journal of Industrial Ergonomics, 35*(4), 307-320.

Ergan, S., Radwan, A., Zou, Z., Tseng, H.-a., & Han, X. (2019). Quantifying Human Experience in Architectural Spaces with Integrated Virtual Reality and Body Sensor Networks. *Journal of Computing in Civil Engineering, 33*(2), 04018062.

Filippi, C., Choi, Y. B., Fox, N. A., & Woodward, A. L. (2020). Neural correlates of infant action processing relate to theory of mind in early childhood. *Dev Sci, 23*(2), e12876.

Fine, S., Singer, Y., & Tishby, N. (1998). The hierarchical hidden Markov model: Analysis and applications. *Machine Learning, 32*(1), 41-62.

Flach, A., Memon, A., Lau, S. L., & David, K. (2011). *Pedestrian Movement Recognition for Radio Based Collision Avoidance: A Performance Analysis*. Paper presented at the Proceedings of the 73rd IEEE Vehicular Technology Conference, Budapest, Hungary.

Flores, C., Merdrignac, P., de Charette, R., Navas, F., Milanés, V., & Nashashibi, F. (2019). A Cooperative Car-Following/Emergency Braking System With Prediction-Based Pedestrian Avoidance Capabilities. *IEEE Transactions on Intelligent Transportation Systems, 20*(5), 1837-1846.

Foxe, J., & Snyder, A. (2011). The Role of Alpha-Band Brain Oscillations as a Sensory Suppression Mechanism during Selective Attention. *Frontiers in Psychology, 2*(154).

Frampton, R. J., & Millington, J. E. (2022). Vulnerable Road User Protection from Heavy Goods Vehicles Using Direct and Indirect Vision Aids. *Sustainability, 14*(6).

Friedman, M. (1937). The Use of Ranks to Avoid the Assumption of Normality Implicit in the Analysis of Variance. *Journal of the American Statistical Association, 32*(200), 675-701.

Frith, C., & Dolan, R. (1996). The role of the prefrontal cortex in higher cognitive functions. *Brain Res Cogn Brain Res, 5*(1-2), 175-181.

Fu, T., Hu, W., Miranda-Moreno, L., & Saunier, N. (2019). Investigating secondary pedestrian-vehicle interactions at non-signalized intersections using vision-based trajectory data. *Transportation Research Part C: Emerging Technologies, 105*, 222-240.

Fu, T., Miranda-Moreno, L., & Saunier, N. (2018). A novel framework to evaluate pedestrian safety at non-signalized locations. *Accident Analysis & Prevention, 111*, 23-33.

Gandhi, T., & Trivedi, M. (2007). Pedestrian Protection Systems: Issues, Survey, and Challenges. *IEEE Transactions on Intelligent Transportation Systems, 8*, 413-430.

Gannouni, S., Aledaily, A., Belwafi, K., & Aboalsamh, H. (2021). Emotion detection using electroencephalography signals and a zero-time windowing-based epoch estimation and relevant electrode identification. *Scientific Reports, 11*(1), 7071.

Gao, N., Zhao, L., & Ieee. (2016). *A Pedestrian Dead Reckoning System using SEMG based on Activities Recognition*. Paper presented at the 2016 IEEE CHINESE GUIDANCE, NAVIGATION AND CONTROL CONFERENCE (CGNCC).

Gao, Q., Zhao, X., Yu, X., Song, Y., & Wang, Z. (2018). Controlling of smart home system based on brain-computer interface. *Technol Health Care, 26*(5), 769-783.

Gerogiannis, A., & Bode, N. W. F. (2024). Analysis of long-term observational data on pedestrian road crossings at unmarked locations. *Safety Science, 172*, 106420.

Ghomi, H., & Hussein, M. (2022). An integrated text mining, literature review, and meta-analysis approach to investigate pedestrian violation behaviours. *Accident Analysis and Prevention, 173*.

Goldhammer, M., Koehler, S., Zernetsch, S., Doll, K., Sick, B., & Dietmayer, K. (2018). Intentions of Vulnerable Road Users - Detection and Forecasting by Means of Machine Learning. *IEEE Transactions on Intelligent Transportation Systems*.

Gramfort, A., Luessi, M., Larson, E., Engemann, D. A., Strohmeier, D., Brodbeck, C., Goj, R., Jas, M., Brooks, T., Parkkonen, L., & Hämäläinen, M. (2013). MEG and EEG data analysis with MNE-Python. *Frontiers in Neuroscience, 7*.

Haleem, K., Alluri, P., & Gan, A. (2015). Analyzing pedestrian crash injury severity at signalized and non-signalized locations. *Accident Analysis & Prevention, 81*, 14-23.

Harle, R. (2013). A Survey of Indoor Inertial Positioning Systems for Pedestrians. *IEEE COMMUNICATIONS SURVEYS AND TUTORIALS, 15*(3), 1281-1293.

He, H., Bai, Y., Garcia, E., & Li, S. (2008). *ADASYN: Adaptive Synthetic Sampling Approach for Imbalanced Learning*. Paper presented at the IEEE International Joint Conference on Neural Networks.

Helfrich, R. F., Huang, M., Wilson, G., & Knight, R. T. (2017). Prefrontal cortex modulates posterior alpha oscillations during top-down guided visual perception. *114*(35), 9457-9462.

Homburger, W. S., Keefer, L. E., McGrath, W. R., & Institute of Transportation, E. (1982). *Transportation and traffic engineering handbook* (2nd ed ed.). Englewood Cliffs, N.J.: Prentice-Hall.

Huang, C., Lv, C., Hang, P., Hu, Z., & Xing, Y. (2021). Human-Machine Adaptive Shared Control for Safe Driving Under Automation Degradation. *IEEE Intelligent Transportation Systems Magazine*, 2-15.

Jensen, O., Kaiser, J., & Lachaux, J.-P. (2007). Human gamma-frequency oscillations associated with attention and memory. *Trends in neurosciences, 30*, 317-324.

Jiang, T., Fang, Y., Zheng, N., & Chen, J. (2024). Understanding construction workers' cognitive processes under risky scenarios through electroencephalography. *Automation in Construction, 166*, 105674.

Jiang, Z. C., Song, G., Qian, Y., & Wang, Y. (2022). A deep learning framework for detecting and localizing abnormal pedestrian behaviors at grade crossings. *Neural Computing & Applications, 34*(24), 22099-22113.

Kalantarov, S., Riemer, R., & Oron-Gilad, T. (2018). Pedestrians' road crossing decisions and body parts' movements. *Transportation Research Part F: Traffic Psychology and Behaviour, 53*, 155-171.

Karakaş, S. (2020). A review of theta oscillation and its functional correlates. *International Journal of Psychophysiology*.

Keller, C., & Gavrila, D. (2014). Will the Pedestrian Cross? A Study on Pedestrian Path Prediction. *Intelligent Transportation Systems, IEEE Transactions on, 15*, 494-506.

Kim, J. (2023). U.S. pedestrian deaths reach a 40-year high. Retrieved from https://www.npr.org/2023/06/26/1184034017/us-pedestrian-deaths-high-traffic-car

Kim, U.-H., Ka, D., Yeo, H., & Kim, J.-H. (2020). A Real-time Vision Framework for Pedestrian Behavior Recognition and Intention Prediction at Intersections Using 3D Pose Estimation. *arXiv, abs/2009.10868*.

Klem, G. H., Lüders, H. O., Jasper, H. H., & Elger, C. (1999). The ten-twenty electrode system of the International Federation. The International Federation of Clinical Neurophysiology.

Electroencephalogr Clin Neurophysiol Suppl, 52, 3-6.

Koda, Y., Nakashima, K., Yamamoto, K., Nishio, T., Morikura, M., & Ieee. (2020, Jan 10-13). *Cooperative Sensing in Deep RL-Based Image-to-Decision Proactive Handover for mmWave Networks.* Paper presented at the IEEE 17th Annual Consumer Communications and Networking Conference (CCNC), Las Vegas, NV.

Koehler, S., Goldhammer, M., Bauer, S., Zecha, S., Doll, K., Brunsmann, U., & Dietmayer, K. (2013). Stationary Detection of the Pedestrian?s Intention at Intersections. *IEEE Intelligent Transportation Systems Magazine, 5*(4), 87-99.

Koopmann, B., Puch, S., Ehmen, G., & Fränzle, M. (2020, May 02-04). *Cooperative Maneuvers of Highly Automated Vehicles at Urban Intersections: A Game-theoretic Approach.* Paper presented at the 6th International Conference on Vehicle Technology and Intelligent Transport Systems (VEHITS), Electr Network.

Kowalski-Trakofler, K. M., & Barrett, E. A. (2003). The concept of degraded images applied to hazard recognition training in mining for reduction of lost-time injuries. *Journal of Safety Research, 34*(5), 515-525.

Kuipers, B. (2020). 420421Perspectives on Ethics of AI: Computer Science. In M. D. Dubber, F. Pasquale, & S. Das (Eds.), *The Oxford Handbook of Ethics of AI* (pp. 0): Oxford University Press.

Kumar, A., & Ghosh, I. (2022). Non-compliance behaviour of pedestrians and the associated conflicts at signalized intersections in India. *Safety Science, 147*, 105604.

Kumar, A., Paul, M., & Ghosh, I. (2019). Analysis of Pedestrian Conflict with Right-Turning Vehicles at Signalized Intersections in India. *Journal of Transportation Engineering, Part A: Systems, 145*(6), 04019018.

Liao, L.-D., Chen, C.-Y., Wang, I. J., Chen, S.-F., Li, S.-Y., Chen, B.-W., Chang, J.-Y., & Lin, C.-T. (2012). Gaming control using a wearable and wireless EEG-based brain-computer interface device with novel dry foam-based sensors. *Journal of Neuroengineering and Rehabilitation, 9*(1), 5.

Liao, P.-C., Zhou, X., Chong, H.-Y., Hu, Y., & Zhang, D. (2022). Exploring construction workers' brain connectivity during hazard recognition: a cognitive psychology perspective. *International journal of occupational safety and ergonomics : JOSE*, 1-9.

Liebner, M., Klanner, F., & Stiller, C. (2013). *Active safety for vulnerable road users based on smartphone position data*. Paper presented at the Intelligent Vehicles Symposium (IV).

Lipovac, K., Vujanic, M., Maric, B., & Nesic, M. (2013). Pedestrian Behavior at Signalized Pedestrian Crossings. *Journal of Transportation Engineering, 139*(2), 165-172.

Lu, Y., & Bi, L. (2019). EEG Signals-Based Longitudinal Control System for a Brain-Controlled Vehicle. *IEEE Trans Neural Syst Rehabil Eng, 27*(2), 323-332.

Lyu, W., Mun Lee, Y., Uzondu, C., Madigan, R., Gonçalves, R. C., Garcia de Pedro, J., Romano, R., & Merat, N. (2024). A distributed simulation study to investigate pedestrians' road-crossing decisions and head movements in response to different vehicle kinematics in mixed traffic. *Transportation Research Part F: Traffic Psychology and Behaviour, 104*, 1-14.

Malik, S., Khan, M., Khan, M., & El-Sayed, H. (2023). Collaborative Perception—The Missing Piece in Realizing Fully Autonomous Driving. *Sensors, 23*.

Maoz, U., Yaffe, G., Koch, C., & Mudrik, L. (2019). Neural precursors of decisions that matter—an ERP study of deliberate and arbitrary choice. *eLife, 8*, e39787.

Markkula, G., Madigan, R., Nathanael, D., Portouli, E., Lee, Y. M., Dietrich, A., Billington, J., Schieben, A., & Merat, N. (2020). Defining interactions: a conceptual framework for understanding interactive behaviour in human and automated road traffic. *Theoretical Issues in Ergonomics Science, 21*(6), 728-752.

Martínez-Vázquez, P., & Gail, A. (2018). Directed Interaction Between Monkey Premotor and Posterior Parietal Cortex During Motor-Goal Retrieval from Working Memory. *Cerebral Cortex, 28*(5), 1866-1881.

Matsui, Y., Hitosugi, M., Takahashi, K., & Doi, T. (2013). Situations of Car-to-Pedestrian Contact. *Traffic injury prevention, 14*, 73-77.

McIntosh, J. R., & Sajda, P. (2020). Decomposing Simon task BOLD activation using a drift-diffusion model framework. *Scientific Reports, 10*(1), 3938.

Mcity. Mcity Test Facility - University of Michigan. Retrieved from https://mcity.umich.edu/what-we-do/mcity-test-facility/

MNE-Python. mne.time_frequency.tfr_multitaper. Retrieved from https://mne.tools/1.8/generated/mne.time_frequency.tfr_multitaper.html

Mole, C. D., & Wilkie, R. M. (2017). Looking forward to safer HGVs: The impact of mirrors on driver reaction times. *Accident Analysis and Prevention, 107*, 173-185.

Moradi-Pari, E., Tian, D. Y., Mahjoub, H. N., & Bai, S. (2022). The Smart Intersection: A Solution to Early-Stage Vehicle-to-Everything Deployment. *IEEE Intelligent Transportation Systems Magazine, 14*(5), 88-102.

Neogi, S., Hoy, M., Dang, K., Yu, H., & Dauwels, J. (2020). Context Model for Pedestrian Intention Prediction Using Factored Latent-Dynamic Conditional Random Fields. *IEEE Transactions on Intelligent Transportation Systems*, 1-12.

Noh, B., Ka, D., Lee, D., & Yeo, H. (2021). Analysis of Vehicle–Pedestrian Interactive Behaviors near Unsignalized Crosswalk. *Transportation Research Record: Journal of the Transportation Research Board, 2675*, 036119812199906.

Noh, B., No, W., Lee, J., & Lee, D. (2020). Vision-Based Potential Pedestrian Risk Analysis on Unsignalized Crosswalk Using Data Mining Techniques. *Applied Sciences, 10*(3). doi:10.3390/app10031057

Noh, B., Park, H., Lee, S., & Nam, S.-H. (2022). Vision-Based Pedestrian's Crossing Risky Behavior Extraction and Analysis for Intelligent Mobility Safety System. *Sensors, 22*, 3451.

Ojala, M., & Garriga, G. C. (2009, 6-9 Dec. 2009). *Permutation Tests for Studying Classifier Performance.* Paper presented at the 2009 Ninth IEEE International Conference on Data Mining.

Olszewski, P., Szagała, P., Wolański, M., & Zielińska, A. (2015). Pedestrian fatality risk in accidents at unsignalized zebra crosswalks in Poland. *Accident Analysis & Prevention, 84*, 83-91.

Pang, Y., Zhao, X., Yan, H., & Liu, Y. (2021). Data-driven trajectory prediction with weather uncertainties: A Bayesian deep learning approach. *Transportation Research Part C: Emerging Technologies, 130*, 103326.

Papadimitriou, E., Lassarre, S., & Yannis, G. (2016). Introducing human factors in pedestrian crossing behaviour models. *Transportation Research Part F: Traffic Psychology and Behaviour, 36*, 69-82.

Parés-Pujolràs, E., Matić, K., & Haggard, P. (2023). Feeling ready: neural bases of prospective motor readiness judgements. *Neuroscience of Consciousness, 2023*(1).

Peirce, J., Gray, J. R., Simpson, S., MacAskill, M., Höchenberger, R., Sogo, H., Kastman, E., & Lindeløv, J. K. (2019). PsychoPy2: Experiments in behavior made easy. *Behavior Research Methods, 51*(1), 195-203.

Pfurtscheller, G. (1977). Graphical display and statistical evaluation of event-related desynchronization (ERD). *Electroencephalogr Clin Neurophysiol, 43*(5), 757-760.

Pfurtscheller, G. (1992). Event-related synchronization (ERS): an electrophysiological correlate of cortical areas at rest. *Electroencephalogr Clin Neurophysiol, 83*(1), 62-69.

Pfurtscheller, G., & Lopes da Silva, F. H. (1999). Event-related EEG/MEG synchronization and desynchronization: basic principles. *Clinical Neurophysiology, 110*(11), 1842-1857.

Polanía, R., Paulus, W., & Nitsche, M. (2012). Noninvasively Decoding the Contents of Visual Working Memory in the Human Prefrontal Cortex within High-gamma Oscillatory Patterns. *Journal of Cognitive Neuroscience, 24*, 304-314.

Pool, E., Kooij, J., & Gavrila, D. (2017). *Using road topology to improve cyclist path prediction*. Paper presented at the IEEE Intelligent Vehicles Symposium (IV).

Ptak, R. (2012). The Frontoparietal Attention Network of the Human Brain: Action, Saliency, and a Priority Map of the Environment. *Neuroscientist, 18*(5), 502-515.

Puga, J., Meneses, F., Moreira, A., & Ieee. (2023, Jun 20-23). *On the Feasibility of Using 5G Enabled Smartphones to Improve Safety of Vulnerable Road Users.* Paper presented at the 97th IEEE

Vehicular Technology Conference (VTC-Spring), Florence, ITALY.

Rabiner, L. R. (1989). A tutorial on hidden Markov models and selected applications in speech recognition. *Proceedings of the IEEE, 77*(2), 257-286.

Rasouli, A., Kotseruba, I., & Tsotsos, J. K. (2018). Understanding Pedestrian Behavior in Complex Traffic Scenes. *IEEE Transactions on Intelligent Vehicles, 3*(1), 61-70.

Ratanamahatana, C. A., & Keogh, E. (2005). Three Myths about Dynamic Time Warping Data Mining. In *Proceedings of the 2005 SIAM International Conference on Data Mining (SDM)* (pp. 506-510).

Rehder, E., & Kloeden, H. (2015). *Goal-Directed Pedestrian Prediction*. Paper presented at the IEEE International Conference on Computer Vision Workshop (ICCVW).

Rich, M. (2020). Rolling Zettabytes: Quantifying the Data Impact of Connected Cars. Retrieved from https://www.datacenterfrontier.com/connected-cars/article/11429212/rolling-zettabytes-quantifying-the-data-impact-of-connected-cars

Ridel, D., Rehder, E., Lauer, M., Stiller, C., & Wolf, D. (2018, 4-7 Nov. 2018). *A Literature Review on the Prediction of Pedestrian Behavior in Urban Scenarios*. Paper presented at the 2018 21st International Conference on Intelligent Transportation Systems (ITSC).

Rothenbücher, D., Li, J., Sirkin, D., Mok, B., & Ju, W. (2016, 26-31 Aug. 2016). *Ghost driver: A field study investigating the interaction between pedestrians and driverless vehicles*. Paper presented at the 2016 25th IEEE International Symposium on Robot and Human Interactive Communication (RO-MAN).

Sakoe, H., & Chiba, S. (1978). Dynamic programming algorithm optimization for spoken word recognition. *IEEE Transactions on Acoustics, Speech, and Signal Processing, 26*(1), 43-49.

Salazar-Gomez, A., DelPreto, J., Gil, S., Guenther, F., & Rus, D. (2017). *Correcting robot mistakes in real time using EEG signals*.

Saleh, K., Hossny, M., & Nahavandi, S. (2017, 16-19 Oct. 2017). *Intent prediction of vulnerable road users from motion trajectories using stacked LSTM network*. Paper presented at the 2017 IEEE 20th International Conference on Intelligent Transportation Systems (ITSC).

Saleh, K., Hossny, M., & Nahavandi, S. (2018). Intent Prediction of Pedestrians via Motion Trajectories Using Stacked Recurrent Neural Networks. *IEEE Transactions on Intelligent Vehicles*, 1-1.

Saleh, K., Hossny, M., & Nahavandi, S. (2019). Contextual Recurrent Predictive Model for Long-Term Intent Prediction of Vulnerable Road Users. *IEEE Transactions on Intelligent Transportation Systems*, 1-11.

Schmidt, S., & Färber, B. (2009). Pedestrians at the kerb – Recognising the action intentions of humans. *Transportation Research Part F: Traffic Psychology and Behaviour, 12*(4), 300-310.

Schneider, N., & Gavrila, D. (2013). *Pedestrian Path Prediction with Recursive Bayesian Filters: A Comparative Study*. Paper presented at the Proceedings of the 35th German Conference on Pattern Recognition.

Schrouff, J., Raccah, O., Baek, S., Rangarajan, V., Salehi, S., Mourão-Miranda, J., Helili, Z., Daitch, A., & Parvizi, J. (2020). Fast temporal dynamics and causal relevance of face processing in the human temporal cortex. *Nature Communications, 11*.

Sharma, A., Singh, A., Gupta, V., & Arya, S. (2022). Advancements and future prospects of wearable sensing technology for healthcare applications. *Sensors & Diagnostics, 1*(3), 387-404.

Shokri-Kojori, E., Motes, M. A., Rypma, B., & Krawczyk, D. C. (2012). The Network Architecture of Cortical Processing in Visuo-spatial Reasoning. *Scientific Reports, 2*(1), 411.

Slepian, D. (1978). Prolate spheroidal wave functions, fourier analysis, and uncertainty — V: the discrete case. *The Bell System Technical Journal, 57*(5), 1371-1430.

Song, X., Chen, K., Li, X., Sun, J., Hou, B., Cui, Y., Zhang, B., Xiong, G., & Wang, Z. (2020). Pedestrian Trajectory Prediction Based on Deep Convolutional LSTM Network. *IEEE Transactions on Intelligent Transportation Systems*, 1-18.

Steinemann, N. A., O'Connell, R. G., & Kelly, S. P. (2018). Decisions are expedited through multiple neural adjustments spanning the sensorimotor hierarchy. *Nature Communications, 9*(1), 3627.

Sucha, M., Dostal, D., & Risser, R. (2017). Pedestrian-driver communication and decision strategies at

marked crossings. *Accident Analysis & Prevention, 102*, 41-50.

Sugimoto, C., Nakamura, Y., & Hashimoto, T. (2008). *Prototype of pedestrian-to-vehicle communication system for the prevention of pedestrian accidents using both 3G wireless and WLAN communication*. Paper presented at the 3rd International Symposium on Wireless Pervasive Computing.

Sulpizio, V., Lucci, G., Berchicci, M., Galati, G., Pitzalis, S., & Di Russo, F. (2017). Hemispheric asymmetries in the transition from action preparation to execution. *Neuroimage, 148*, 390-402.

Sun, T., & Walsh, C. A. (2006). Molecular approaches to brain asymmetry and handedness. *Nat Rev Neurosci, 7*(8), 655-662.

Swargiary, M., & Kadali, B. R. (2023). A study on meta-analysis approach for pedestrian-vehicle interaction using LiDAR. *Transportation Engineering, 13*, 100191.

Tang, Z. Y., He, J. H., Flanagan, S. K., Procter, P., Cheng, L., & Ieee Comp, S. O. C. (2021, Nov 01-05). *Cooperative Connected Smart Road Infrastructure and Autonomous Vehicles for Safe Driving.* Paper presented at the 29th IEEE International Conference on Network Protocols (ICNP), Electr Network.

Tavenard, R., Faouzi, J., Vandewiele, G., Divo, F., Androz, G., Holtz, C., Payne, M., Yurchak, R., Rußwurm, M., Kolar, K., & Woods, E. (2020). Tslearn, a machine learning toolkit for time series data. *J. Mach. Learn. Res., 21*(1), Article 118.

Tian, K., Markkula, G., Wei, C., Lee, Y. M., Madigan, R., Merat, N., & Romano, R. (2022). Explaining unsafe pedestrian road crossing behaviours using a Psychophysics-based gap acceptance model. *Safety Science, 154*, 105837.

Tsumura, K., Aoki, R., Takeda, M., Nakahara, K., & Jimura, K. (2021). Cross-Hemispheric Complementary Prefrontal Mechanisms during Task Switching under Perceptual Uncertainty. *Journal of Neuroscience, 41*(10), 2197-2213.

Valos, N., & Bennett, J. M. (2023). The relationship between cognitive functioning and street-crossing behaviours in adults: A systematic review and meta-analysis. *Transportation Research Part F: Traffic Psychology and Behaviour, 99*, 356-373.

Värbu, K., Muhammad, N., & Muhammad, Y. (2022). Past, Present, and Future of EEG-Based BCI Applications. *Sensors (Basel), 22*(9).

Vinck, M., Oostenveld, R., van Wingerden, M., Battaglia, F., & Pennartz, C. M. (2011). An improved index of phase-synchronization for electrophysiological data in the presence of volume-conduction, noise and sample-size bias. *Neuroimage, 55*(4), 1548-1565.

Volz, B., Behrendt, K., Mielenz, H., Gilitschenski, I., Siegwart, R., & Nieto, J. (2016). *A data-driven approach for pedestrian intention estimation*. Paper presented at the IEEE 19th International Conference on Intelligent Transportation Systems (ITSC).

Wagner, J., Wessel, J., Ghahremani, A., & Aron, A. (2017). Establishing a Right Frontal Beta Signature for Stopping Action in Scalp Electroencephalography: Implications for Testing Inhibitory Control in Other Task Contexts. *Journal of Cognitive Neuroscience, 30*, 1-12.

Wang, C., Zhang, H., Wang, H., & Fu, R. (2021). The effect of "yield to pedestrians" policy enforcement on pedestrian street crossing behavior: A 3-year case study in Xi'an, China. *Travel Behaviour and Society, 24*, 172-180.

Wang, T.-H., Manivasagam, S., Liang, M., Yang, B., Zeng, W., & Urtasun, R. (2020). V2VNet: Vehicle-to-Vehicle Communication for Joint Perception and Prediction. In *Computer Vision – ECCV 2020* (pp. 605-621).

WHO. (2023). *Road traffic injuries*. Retrieved from https://www.who.int/news-room/fact-sheets/detail/road-traffic-injuries

Windridge, D., Shaukat, A., & Hollnagel, E. (2013). Characterizing Driver Intention via Hierarchical Perception–Action Modeling. *IEEE Transactions on Human-Machine Systems, 43*(1), 17-31.

Yang, H., Ling, Y. F., Kopca, C., Ricord, S., & Wang, Y. H. (2022). Cooperative traffic signal assistance system for non-motorized users and disabilities empowered by computer vision and edge artificial. *Transportation Research Part C-Emerging Technologies, 145*.

Yeong, D. J., Velasco-Hernandez, G., Barry, J., & Walsh, J. (2021). Sensor and Sensor Fusion Technology in Autonomous Vehicles: A Review. *Sensors, 21*, 2140.

Yi, B., Cao, H., Song, X., Wang, J., Guo, W., & Huang, Z. (2023). How human-automation interaction experiences, trust propensity and dynamic trust affect drivers' physiological responses in conditionally automated driving: Moderated moderated-mediation analyses. *Transportation Research Part F: Traffic Psychology and Behaviour, 94*, 133-150.

Yin, Y., Han, J., & Childs, P. R. N. (2024). An EEG study on artistic and engineering mindsets in students in creative processes. *Scientific Reports, 14*(1), 13364.

Yu, X., Chum, P., & Sim, K.-B. (2014). Analysis the effect of PCA for feature reduction in non-stationary EEG based motor imagery of BCI system. *Optik, 125*, 1498-1502.

Yu, Y., Zhou, Z., Liu, Y., Jiang, J., Yin, E., Zhang, N., Wang, Z., Liu, Y., Wu, X., & Hu, D. (2017). Self-Paced Operation of a Wheelchair Based on a Hybrid Brain-Computer Interface Combining Motor Imagery and P300 Potential. *Ieee Transactions on Neural Systems and Rehabilitation Engineering, 25*(12), 2516-2526.

Zafri, N. M., Tabassum, T., Himal, M. R. H., Sultana, R., & Debnath, A. K. (2022). Effect of pedestrian characteristics and their road crossing behaviors on driver yielding behavior at controlled intersections. *Journal of Safety Research, 81*, 1-8.

Zhang, Q., Liang, M., Chan, A. P. C., & Liao, P.-C. (2023). Visual attention and cognitive process in construction hazard recognition: Study of fixation-related potential. *Automation in Construction, 148*, 104756.

Zou, Z., Ergan, S., Fisher-Gewirtzman, D., & Curtis, C. (2021). Quantifying the Impact of Urban Form on Human Experience: Experiment Using Virtual Environments and Electroencephalogram. *Journal of Computing in Civil Engineering, 35*(3), 04021004.